6G for Connected Sky

"6G-SKY"

Work Package 2:

Multi-Technology Connectivity Links

Deliverable D2.1:

A2A, A2G, NTN HAPs, and NTN Satellite Links for 6G

6G-SKY Project:

- **version 1.0: 2024-09-13**

Abstract

This deliverable provides analysis of selected 6G links for air-to-air (A2A), air-to-ground (A2G), high altitude platform stations (HAPS), and non-terrestrial networks (NTN) satellite link communications. This report includes analysis of NTN satellite links from low earth orbit (LEO), medium earth orbit (MEO) and geostationary earth orbit (GEO) satellites serving as HAPS backhaul link. Analysis of links from HAPS to ground users focuses on providing coverage on rural areas, while analysis of A2G links between terrestrial base station and airborne users focuses on personal aerial vehicles and unmanned aerial vehicles (UAVs). A2A links are analyzed on the context of multi-technology links to serve UAVs. This report also analyzes free-space optics for use in Inter Satellite Links (ISL), Inter HAPS Links, links between satellites and HAPS and orbit-to-ground links (also called Direct To Earth (DTE)).

Participants in WP 2:

- Deutsche Telekom (WPL, TL)
- Ericsson AB, Sweden (TL)
- KTH
- Fraunhofer
- Airbus
- Ericsson Antenna Systems, Germany (TL)

6G-SKY, Work Package 2: Multi-Technology Connectivity Links

Task T2.1: High capacity 6G A2A and A2G links enabled by mix of radio technologies

Task T2.3: NTN HAP and satellite links

D2.1: A2A, A2G, NTN HAPs, and NTN Satellite Links for 6G

Editors: Ramon Delgado Pulgar - EAB
Jozef Mindok - DT

Reviewer: Thomas Heyn – Fraunhofer IIS

Contributors: See list of authors

6G-SKY

Deliverable 2.1: A2A, A2G, NTN HAPs, and NTN Satellite Links for 6G

- Editors: Ramon Delgado Pulgar, Ericsson AB
  Jozef Mindok, Deutsche Telekom
- Project coordinator: Dominic Schupke, Airbus
- Technical Project coordinator: Cicek Cavdar, KTH
- CELTIC published project result

2022 CELTIC-NEXT participants in project (acronym):

Ericsson AB	Ericsson Hungary
Ericsson Antenna Systems	Airbus
KTH	PTS
SAS	Deutsche Telekom (DT)
Fraunhofer	Lakeside Labs
RED Bernard	Logistik Center Austria Süd
AITIA	TWINS
Meshmerize	Skysense
Motius	

Document History

Version	Date	Author(s)/Reviewer	Comment
v0.3	2024-07-19	Thomas Heyn, Fraunhofer (reviewer)	
v1.0	2024-09-13	Ramon Delgado Pulgar (editor)	

Executive Summary

This deliverable provides analysis of selected 6G links for air-to-air (A2A), air-to-ground (A2G) and non-terrestrial networks (NTN) such as satellite and high altitude platform stations (HAPS) link communications.

The various links in a 3D architecture of combined Airspace and NTN (ASN) must overcome different challenges to satisfy the emerging new services provided by both terrestrial networks (TN) and NTN. This report defines and describes best link parameters and antenna systems for various communication channels.

First, this deliverable presents an overview of links present in a 3D network architecture, highlighting selected links that are analyzed in the subsequent sections. An overview of existing and envisioned spectrum candidates is also included for the multiple bands to be considered for each link. For selected links in the 3D architecture, a discussion on key performance indicators and performance characteristics is considered, with a focus on providing realistic values.

This report includes analysis of NTN satellite links from low earth orbit (LEO), medium earth orbit (MEO) and geostationary earth orbit (GEO) satellites with a focus on serving ground users. Analysis of links from HAPS to ground users focuses on providing mobile broadband coverage for rural areas. A2G links between terrestrial base station and airborne users are studied with a focus on personal aerial vehicles, like flying taxis, and unmanned aerial vehicles (UAVs). A2A links are analyzed on the context of multi-technology links to serve UAVs. This report also analyzes free-space optics for use in Inter Satellite Links (ISL), Inter HAP Links, and HAPS and orbit-to-ground links (also called Direct To Earth (DTE)).

New technological advancements are needed to enable ubiquitous coverage by a 3D network architecture. These technological advancements cover several aspects of telecommunication networks, including development of new antenna technology, identifying potential spectrum candidates for 6G, and ensure efficient use of spectrum by using best link parameters to connect aerial users and platforms. Enhancement to resilience for end users can be obtained by using multi-link connectivity. To satisfy capacity requirements, free-space optics technology can be used for several NTN link, like inter-satellite links and feeder links.

List of Authors

Name	Affiliation
Bastian Bertholdt	Airbus
Ramon Delgado Pulgar	Ericsson AB
Hieu Do	Ericsson AB
Gabor Fodor	Ericsson AB
Leo Frank	Fraunhofer IIS
Jozef Mindok	Deutsche Telekom
Veli-Matti Riepula	Deutsche Telekom
Mustafa Özger	KTH

Table of Contents

Contents

Glossary

List of acronyms with alphabetical order.

3GPP	Third Generation Partnership Project
5G	Fifth-generation of cellular networks
6G	Sixth-generation of cellular networks
A2A	Air to air
A2G	Air to ground
AAS	Advanced antenna system
ASN	Airspace and NTN
AUE	Aerial UE
AV	Aerial vehicles
BS	Base station
CNR	Carrier to Noise Ratio
CoMP	Coordinated multi-point
CSI	Channel state information
DA2G	Direct air to ground
DL	Downlink
DTE	Direct To Earth
E2E	End to end
EIRP	Effective isotropic radiated power
eVTOL	Electric vertical take-off and landing
FDD	Frequency division duplexing
FSO	Free space optics
FWA	Fixed wireless access
GEO	Geostationary Earth orbit
HAPS	High-altitude platform station
HIBS	HAPS as IMT base station
IoT	Internet of Things
ITU	International Telecommunications Union
KPI	Key performance indicator

LB	Link Budget
LEO	Low Earth orbit
LOS	Line of sight
MEO	Medium Earth Orbit
MIMO	Multiple-input multiple-output
NLOS	Non-line of sight
NR	New Radio
NTN	Non-terrestrial networks
SAR	Specific Absorption Rate
SINR	Signal to interference and noise ratio
TDD	Time division duplexing
TN	Terrestrial networks
UAM	Urban Air Mobility
UAV	Unmanned aerial vehicle
UE	User equipment
UL	Uplink
UTM	Unmanned traffic management
WP	Work package
WRC	World Radio Conference

1 Introduction

The 6G-Sky project aims at solutions to enable reliable and robust connectivity for aerial and ground users via flexible and adaptive network architecture adopting multiple technologies such as satellites, high altitude platform stations as International Mobile Telecommunications base stations (HIBS), direct air to ground communication (DA2GC) etc. In addition, this project focuses on novel wireless network design and management schemes in 3D space including different types of flying vehicles with their unique requirements. Another focus is to provide robust, low latency and/or high-capacity communications to ground users in the rural areas without any infrastructure via non terrestrial networks (NTNs), which are already initially introduced in 5G [1].

Selected sets of communication technologies used in the multi-layered 3D network architecture are evaluated and the main goal of this work package (WP2) is to define and proof the best link parameters and antenna systems for various communication channels. Link design parameters, particularly capacity, delay, reliability, and availability, are investigated respectively to the links' end points, i.e., on board satellites, HAPS, aircraft, drones/electric vertical take-off and landing vehicles (eVTOLs), and on ground. In addition, prototypes of ground and airborne antennas are designed, developed and assessed.

1.1 Objective of the document

This document gives an overview of all possible communication links in the multi-layered 3D network as depicted on the 6G-Sky reference architecture [Figure 1]. A set of links have been selected based on WP2 partners interest and for this highlighted subset, a detailed study is presented.

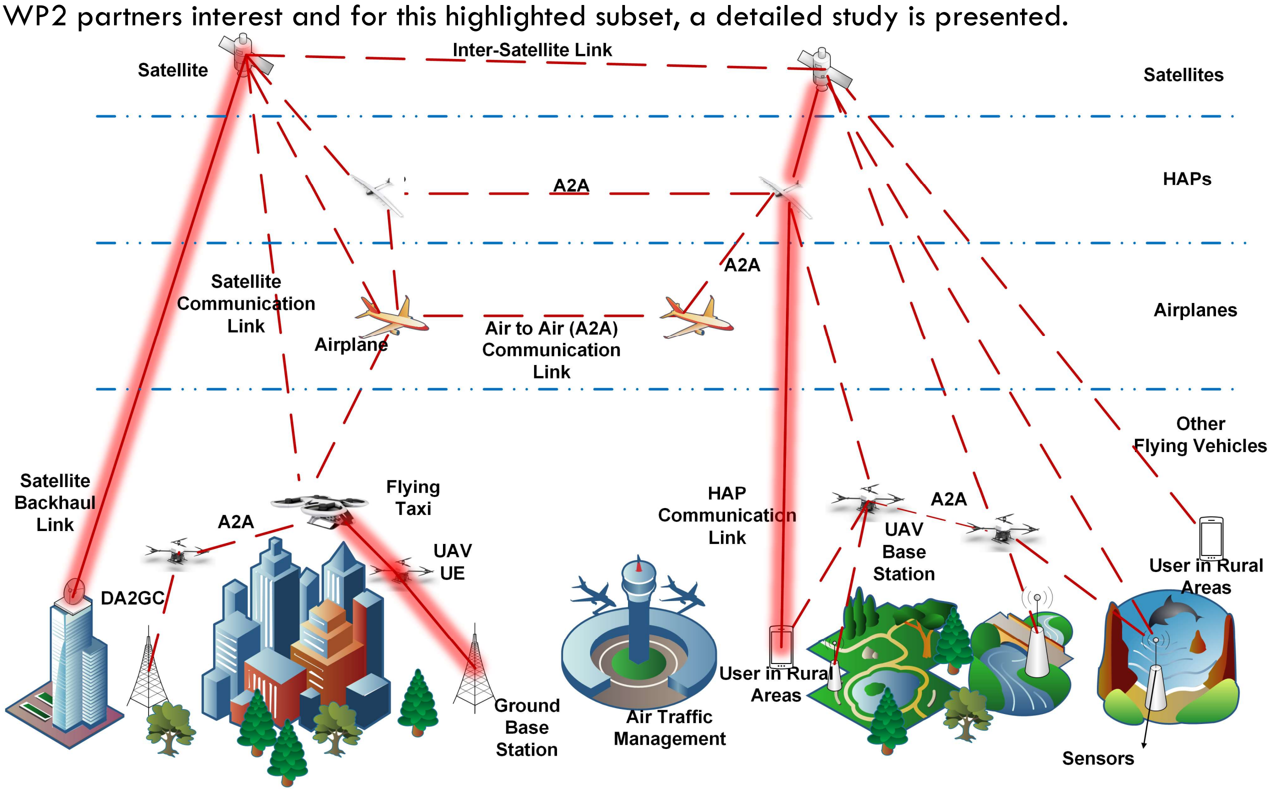

Figure 1 3D Network Architecture

This deliverable has the following main objectives:

- Identification of links of interest, including their foreseen frequency bands.

- Set target key performance indicators (KPIs) and system parameters for selected links.
- Detailed Link budget (LB) calculations and performance analysis.

2 Communication links for a connected sky

This section provides an overview of the links of interest and how do these fit within the context of combined ASN, and identifies spectrum candidates for the respective links.

Table 1 describes usage and role of various aerial and ground elements in a 3D architecture as depicted in Figure 1.

	Typical Use case	Typical Role	Technology	Remarks
GEO/LEO/MEO	Backhaul for extended networks Direct-to-device, as standardized in 3GPP since Rel-17	backhaul for BS	RF, FSO	Free Space Optics (FSO)
HAPS	Broadband	HIBS	RF, FSO	RF for UE link, RF/FSO for backhaul
Aircraft (Airliner)	Broadband	UE	RF	Typically, Inflight Connectivity
H/C, eVTOL, UAV, Small UAVs	Remote UAV controller through High-Definition video; High-Definition patrol and laser mapping	UE	Key technologies for connectivity are massive MIMO and new spectrum with large bandwidth	Main challenges are inter-cell interference when served by terrestrial networks, channel aging due to 3D high mobility of airborne vehicles, and coexistence with NTN satellite, radar and other existing services.
Terrestrial UE	Broadband	UE	RF, based on 3GPP standards	
Terrestrial BS	Provide connectivity at ground level and near ground	BS	RF, massive MIMO, large bandwidth	

Ground Station	Provides feeder link connectivity	Backhaul	RF	Satellite or HAPS feeder link

Table 1 Usage and roles of aerial and ground elements

Links present in the 3D network architecture can be summarized in Table 2, where the links included in this document are highlighted in green. Furthermore, partners' names are indicated by each link based on their area of interest and for which a detailed study has been performed in chapter 4.

Color legend:
Included in the D2.1
In 6G-Sky reference architecture
Out of scope

"Node_1" Antenna/Link of interest	Counterpart "Node_2" terminating the link: GEO	LEO/MEO	HAPS	A/C	eVTOL, UAV, HC	Small UAV's	Terrestrial UE	Terrestrial BS	Ground Station
GEO			DT, Airbus	Airbus	Airbus	Airbus			FhG
LEO/MEO		FhG	DT, Airbus	Airbus	KTH, Airbus	KTH, Airbus	DT, KTH		FhG
HAPS	DT, Airbus	DT, Airbus	DT	DT	DT, KTH	DT, KTH	DT, KTH	DT	DT
A/C	Airbus	Airbus	DT						DT
H/C, eVTOL, UAV	Airbus	Airbus	DT		KTH	KTH		EAB, EAG, KTH	
Small UAV's	Airbus	Airbus	DT		KTH	KTH		EAB, EAG, KTH	
Terrestrial UE		DT	DT						
Terrestrial BS (incl. dedicated uptilt BS)			DT		EAB, EAG, KTH	EAB, EAG, KTH			
Ground Station	FhG	FhG	DT	DT, EAG, KTH					

Table 2 Communications links matrix

Table 3 provides an overview of spectrum candidates that are either already commonly used or are envisioned to be used in the future. It is noted that a multitude of different bands can be considered for each link. For example, a HAPS-to-terrestrial user link can already use 3GPP bands on sub-6 GHz (FR1) for handset type of UEs [2]. FR3 (7-24 GHz) is a potential new spectrum candidate for this link, for which several studies exist and which will be further covered in WRC-27. Both aforementioned bands are included in the detailed analysis in chapter 4, while Q/V band is envisioned for different UE type and different use case and therefore is not included in the analysis (ref. Table 3)

Color legend:
Included in the D2.1
In 6G-Sky reference architecture
Out of scope

"Node_1" Antenna/Link of interest	Counterpart "Node_2" terminating the link								
	GEO	LEO/MEO	HAPS	A/C	H/C, eVTOL, UAV	Small UAVs	Terrrestrial UE	Terrrestrial BS	Ground Station
GEO	Ka, Ku, Q/V, FSO	Ka, Ku, Q/V, FSO	Ka, Ku, Q/V, FSO	Ka, Ku, Q/V, MSS	FR1, FR3, MSS	FR1, FR3, MSS	Ka, Ku, Q/V, MSS		Ka, Ku, Q/V
LEO/MEO	Ka, Ku, Q/V, FSO	Ka, Ku, Q/V, FSO	Ka, Ku, Q/V, FSO	Ka, Ku, Q/V, MSS	FR1, FR3, MSS	FR1, FR3, MSS	Ka, Ku, Q/V, FR1, FR3, MSS		Ka, Ku, Q/V
HAPS	Ka, Ku, Q/V, FSO	Ka, Ku, Q/V, FSO	Q/V, FSO	Q/V, FR3	FR1, FR3	FR1, FR3	FR1, FR3, Q/V	Q/V	Q/V
A/C	Ka, Ku, Q/V, MSS	Ka, Ku, Q/V, MSS	Q/V, FR3						MSS, FR3
H/C, eVTOL, UAV	FR1, FR3, MSS	FR1, FR3, MSS	FR1, FR3		FR1, FR3	FR1, FR3	FR1, FR3	FR1, FR3	
Small UAVs	FR1, FR3, MSS	FR1, FR3, MSS	FR1, FR3		FR1, FR3	FR1, FR3	FR1, FR3	FR1, FR3	
Terrrestrial UE	Ka, Ku, Q/V, MSS	Ka, Ku, Q/V, FR1, FR3, MSS	FR1, FR3, Q/V		FR1, FR3	FR1, FR3			
Terrrestrial BS			Q/V		FR1, FR3	FR1, FR3			
Ground Station	Ka, Ku, Q/V	Ka, Ku, Q/V	Q/V	MSS, FR3					

FR1: 410MHz-7.125 GHz	3GPP TS 38.101-1
FR3: 7.125-24.25 GHz	
FR2: 24.25-71.00 GHz	3GPP TS 38.101-2
Ku 12.4-18 GHz	
Ka: 26.5-40 GHz	
Q/V: 33-75GHz	
MSS: 1.5-2.5GHz	
FSO: >100 THz	

Table 3 Envisioned spectrum candidates

The satellite frequencies are defined in 3GPP TS 38.101-5, where L-and S-band frequencies are specified. The specification includes as well the FR2-NTN frequency band and it also includes a part of the Ku-band frequencies and is defined from 17300 MHz to 30000 MHz.

3 Key performance indicators for a connected sky

Tables presented in chapter 2 provide a matrix of possible physical links. Each link can be used for a number of different use cases, having different KPI requirements for end-to-end (E2E) latency, reliability, bandwidth etc. On top, some KPIs may only be reached in Line of Sight (LOS) conditions, which is a general assumption for all A2A and A2G communication links.

Target KPIs are estimated based on current state of the art in 5G timeline, see, e.g., [3], with outlook to 6G timeframe. We tried to set the 6G KPIs values to realistic figures rather than aiming for some overestimated and technologically unreachable targets.

For example, for the HAPS-to-UE link, the target KPIs for 5G timeframe are representative of real-life HAPS experiments performed by DT. For 6G timeframe, we have set target KPIs that aim to provide 5x throughput improvement over the set 5G KPIs.

Table 4 shows a summary of 6G KPI requirements for selected links and more detailed KPI requirements can be found in Annex 8.1.

Link	**DL / UL Peak Data Rate**	**E2E Latency**	**Reliability**
HAPS - UE	1000 / 100 Mbps	10 ms	99.99 %
Terrestrial BS - airborne UE	100 / 120 Mbps	20 ms UL/ 100 ms DL	99.9 %
HAPS - GEO	790 / 325 Mbps	142 ms	
HAPS - MEO	740 / 440 Mbps	37 ms	
HAPS - LEO	660 / 510 Mbps	7 ms	
HAPS - HAPS	100 Gbps	1 ms	99.9 %
Ground station - GEO	2 / 8 Gbps	541 ms (max. transparent)	99.99 %
Ground station - LEO	1.06 / 37.1 Gbps		99.99 %

Table 4 Summary of 6G KPI requirements

3.1 Satellite Feeder Links

For the satellite backhaul scenario important KPIs are coverage, data rate and latency. Reducing the latency can be done by using LEO satellites instead of GEO or MEO satellites. If the satellite is regenerative the speed of the hardware and the on-board CPU is important to reduce the end-to-end latency.

Regarding the data rate a high bandwidth and powerful antennas and also BUC and LNB that are connected with relatively low losses as well as aspects like antenna pointing accuracy are playing a big role.

Coverage can be achieved with more satellites or higher orbits.

3.1.1 Ground station to GEO satellites

As shown in Figure 1, the satellites are used to transmit signals to other satellites, HAPS, flying taxis, airplanes and UAVs via an RF or an optical link. In addition, a direct connection to users in rural areas should also be possible as defined in 3GPP (TR 38.821).

The task of the feeder links is to provide the required data from the core network to the user equipment and vice versa. Determining the need for required data rates is very complex because the number of HAPS, UAVs and airplanes that should be connected via a satellite is not specified. The number of feeder links per satellite must therefore be designed as required so that they do not become a bottleneck. For this reason, the specification for GEO satellites is made for one feeder link and not for a specific number of feeder links per satellite. The feeder links for a satellite can be established via one or several ground stations that are on different locations. Several gateways can be set up per ground station and, with the help of circular polarization (RHCP and LHCP), the available frequencies can be used with a frequency reuse factor of two.

For the 5G timeframe (transparent satellites —> 5G NR as air interface) it should be possible to achieve a spectral efficiency of 4 bit/s/Hz and with the bandwidth of 500 MHz in the Ka-band to obtain a data rate of 2 Gbit/s per UL feeder link. As shown in Figure 2 below therefore an SNR of ~16.5 dB is required to achieve the spectral efficiency of 4 bit/s/Hz.

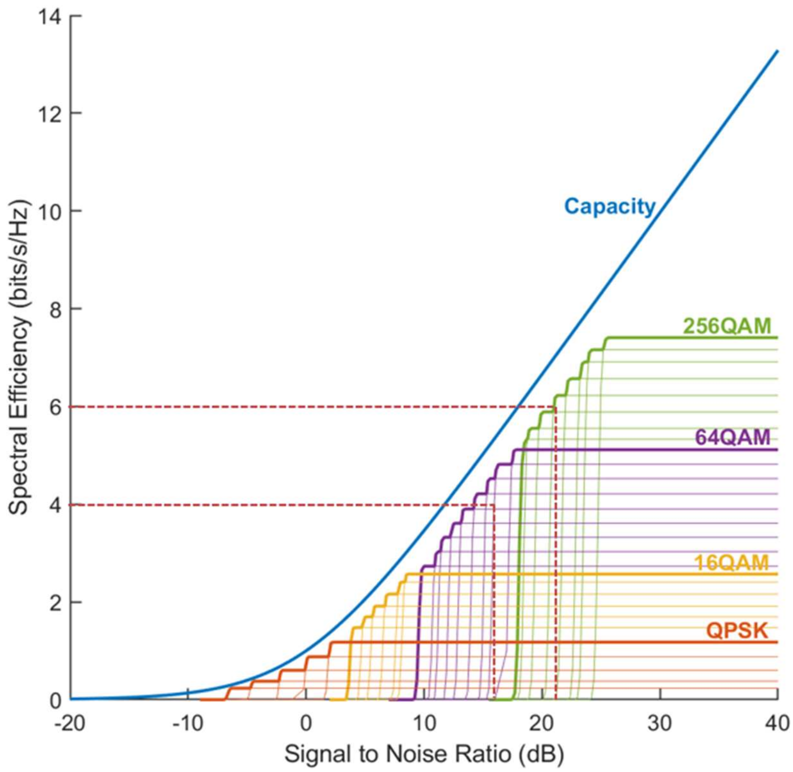

Figure 2 Spectral Efficiency of 5G NR, simulated by Fraunhofer IIS, based on the ALIX Link Level Simulation Tool. Overhead by reference symbols etc. is not taken into account[1]

$$UL\_data\_rate\_5G = 2\ \frac{Gbit}{s}$$

Depending on the use case, the ratio between the uplink and downlink data rate in the user link can vary. In conventional satellite communication, the ratio of the UL and DL data rate in the user link is 1:4. The ratio in the feeder link should therefore be 4:1. The following value can therefore be assumed for the DL data rate:

$$DL\_data\_rate\_5G = UL\_data\_rate\_5G\ /4\ = 0.5\ \frac{Gbit}{s}$$

The higher the required total data rate for the feeder link is, the more parallel links must be implemented. For example, if a data rate of 20 Gbit/s is required in the uplink feeder link, a total of 5 gateway-to-satellite links with 500 MHz bandwidth each with two polarizations must be implemented (5x 500 MHz x2 = 5000 MHz).

Since the Ka-band is heavily used and the bandwidth is limited to 500 MHz, the Q/V band is assumed for the feeder links in the 6G timeframe. The available carrier bandwidths in the Q/V frequency band are up to 2 GHz. Assuming that the higher atmospheric losses in the Q/V compared to the Ka-band can be compensated with technical progress, the following data rates can be expected for the 6G timeframe:

[1] Overhead factor in 3GPP TS 38.306 is 0.14 for frequency range FR1 for DL, 0.18 for frequency range FR2 for DL, 0.08 for frequency range FR1 for UL 0.10, for frequency range FR2 for UL

$$UL\_data\_rate\_6G = 8\ \frac{Gbit}{s}$$

$$DL\_data\_rate\_6G = UL\_data\_rate\_6G\ /4\ = 2\ \frac{Gbit}{s}$$

3.1.2 Ground station to LEO satellites

In contrast to the GEO satellites, several sets (1-1, 1-2 and 1-3) were defined for LEO 600 satellites as part of 3GPP TSG RAN WG1 #116. In addition to the maximum EIRP per satellite beam, the total number of simultaneously active beams (16 to 106) was defined. In combination with the specified data rates (2 Mbit/s for UL and 70 Mbit/s for DL) from ITU-R M.2514-0, a minimum feeder uplink and downlink data rate can be calculated for the 5G timeframe.

$$DL\_data\_rate\_5G = 2\ \frac{Mbit}{s}\ x\ (16\ to\ 106\ beams\ ) = 32\ \frac{Mbit}{s}\ to\ 212\ \frac{Mbit}{s}$$

$$UL\_data\_rate\_5G = 70\ \frac{Mbit}{s}\ x\ (16\ to\ 106\ beams) = 1.2\ \frac{Gbit}{s}\ to\ 7.42\ \frac{Gbit}{s}$$

This is the total data rate that the satellite must provide for the Uu-Link. Additional data streams as for example ISL or the links to HAPS requires higher data rates for the feeder links. As this links are not taken into account the calculated data rate above is a minimum data rate for the feeder links.

A significantly higher required user data rate can be assumed for the 6G timeframe. To ensure a technologically feasible estimate for 6G timeframe, we assume a factor of 5 for both the uplink and downlink data rate. This results in the following specifications for the 6G timeframe feeder link:

$$DL\_data\_rate\_6G\ =\ DL\_data\_rate\_5G\ x\ 5\ =\ 212\ \frac{Mbit}{s}\ x\ 5\ =\ 1.06\ Gbit/s$$

$$UL\_data\_rate\_6G\ =\ UL\_data\_rate\_5G\ x\ 5\ =\ 7.42\ \frac{Gbit}{s}\ x\ 5\ =\ 37.1\ \frac{Gbit}{s}$$

4 Analysis of communication links

4.1 HAPS Satellite Backhaul

This analysis is about the link budget of satellite backhaul scenarios for HAPS via satellites. Therefore, satellites in the three main orbit types LEO, MEO and GEO will be discussed. For this examination the Ka band is considered as the most relevant. Ka band has a wider bandwidth than Ku band and therefore can contain much higher data rates. On the other hand, the Q/V band suffers more losses because of the smaller wave length and higher attenuation e.g., due to rain or clouds. This is the reason why Ka band is considered today as the preferred frequency band for satellite communication.

For the link budget some assumptions were made:

- Assumed maximum elevation angle for HAPS antenna = 30° for GEO, MEO and LEO satellite
- Ka band atmospheric losses = 2.0 dB [5] (adjusted for HAPS height)

- Clear and dry sky conditions
- Assumed 3 dB for implementation penalty
- Latency is one way trip time between Tx/Rx antennas assuming an elevation angle of 30°

The link budget is calculated in the following way:

First the CNR [dB] is calculated:

CNR[dB] = EIRP[dBW] + G/T[dB/K] - k[dBW/K/Hz] - FSPL[dB] - IP[dB] - AL[dB] - BW[dBHz]

With IP ... Implementation Penalty of 3dB

And AL ... Atmospheric losses of 2 dB for Ka band accounting for the height of the HAPS.

With the bandwidth and the CNR, the channel capacity (Shannon limit) C can be calculated:
C = BW*log_2(1+CNR)

For the 5G time frame, three antennas are considered:

Antenna Name	**G/T [dB/K]**	**EIRP [dBW]**
Antenna A (25 W BUC)	11.2	49.0
Antenna B (8 W BUC)	5.2	37.7
Antenna C (25 W BUC)	5.2	42.7

Table 5 Considered antennas; 5G time frame

The assumptions regarding these antennas are as follows:

- High performance state of the art antennas
- Future proof Ka band
- Would fit on HAPS (A, B, C) (e.g. GROB AC, task 5.6)
- Antennas B and C are identical with different BUC

For the 5G time frame, 4 satellites in different orbits are considered:

Antenna Name	**G/T [dB/K]**	**EIRP [dBW]**	**BW [MHz]**	**UL frq [GHz]**	**DL frq [GHz]**
GEO antenna	29.1	72.7	36	20	30
MEO antenna @ 8000 km	21.1	59.7	36	20	30

LEO antenna @ 1200 km	9.1	43.2	36	20	30

Table 6 Considered satellite antennas; 5G time frame

To get a better validity, the approach from the ESA 5G-IS (5G Infrastructure Study) is chosen for this examination.
In that study, the EIRP values are depending on the power flux density on the ground. The power flux density is limited by Radio Regulations to avoid harmful interferences with terrestrial communication systems. The EIRP [dBW] value for each satellite is dependent on the power flux density [dBW/m²] and the bandwidth. So, the EIRP [dBW] values in the table above are calculated for the bandwidth of 36 MHz.
The bandwidth of 36 MHz is a user equipment (satellite terminal on the HAPS) limitation. HAPS currently (that is also the case for the HAPS which will be used in Task 5.6 of this study) must be efficient regarding Size, Weight, and Power (SWaP) parameters to be flexible and perform longer flights. Even though the bandwidth of satellite constellations can be much bigger, the limitation of the user equipment is the reason for the bandwidth of 36 MHz of the satellite backhaul links.

The G/T[dB/K] values were also derived from the 5G-IS. Satellite antenna parameters are depending on the different satellite capabilities, which are typically different for each orbit. Therefore, different G/T[dB/K] values are assumed. High throughput satellites are more likely to be deployed in GEO. GEO satellites are often part of smaller constellations with fewer satellites and have longer lifetimes which is favoring bigger and more capable satellites. Smaller satellites however are more likely to be deployed in LEO. In this orbit many satellites are needed to provide the same coverage. Limited launcher capabilities favor comparatively small satellites.

Even though those power flux density limits are a good base line, which is allowing for a good comparison going forward in this examination, note that this is only a crude first-order approximation as not all frequency bands have a defined PFD limit in ITU Radio Regulations and in practice different values may be agreed upon during the co-ordination process.

For the 6G time frame, it is assumed that HAPS have better SWaP conditions and antenna parameters are getting better by a certain factor. Besides that, all other assumptions that were made above are staying the same.
In this concrete example the bandwidth capabilities of the UE are expanded by the factor three (from 36 MHz to 108 Mhz) and all antenna parameters for satellite antennas and user equipment antennas are advanced by the factor 1.1 compared to the 5G time frame today.

Therefore, the antennas of the user equipment in the 6G time frame are assumed like in this table:

Antenna Name	G/T [dB/K]	EIRP [dBW]
Antenna A 6G (25 W BUC)	11.6	49.4
Antenna B 6G (8 W BUC)	5.6	38.1
Antenna C 6G (25 W BUC)	5.6	43.1

Table 7 Considered antenna; 6G time frame

For the satellite antenna parameters for the 6G time frame are presented in the following table:

Antenna Name	G/T [dB/K]	EIRP [dBW]	BW [MHz]	UL frq [GHz]	DL frq [GHz]
GEO antenna 6G	29.5	77.4	108	20	30
MEO antenna 6G	21.5	64.4	108	20	30
LEO antenna @ 1200 km 6G	9.5	47.9	108	20	30

Table 8 Considered satellite antennas; 6G time frame

4.1.1 Conclusion

In the following tables (Table 9, Table 10 and Table 11) the conclusion of the link budget analysis is presented. The antenna A is the most capable antenna and therefore brings the best results for each orbit. For the beam capacity a frequency reuse factor of 2 is considered.

Satellite backhaul over a GEO satellite:

Parameter	5G time frame KPI Target	6G time frame KPI Target
Peak data rate (user terminated or DL)	260 Mbps	790 Mbps
Peak data rate (user terminated or UL)	150 Mbps	325 Mbps
Experienced user throughput (user terminated or DL)	260 Mbps	790 Mbps
Experienced user throughput (user originated or UL)	150 Mbps	325 Mbps
Beam/cell capacity DL	1444 Mbps	1462 Mbps
Beam/cell capacity UL	833 Mbps	602 Mbps
Total number of Beams/cells DL	500	1000
Total number of Beams/cells UL	500	1000
Minimum elevation angle	30°	30°
Acquisition time	5s to 60s	2s to 20s
UE type	VSAT (25W BUC), BW = 36MHz, Ka band (Antenna A)	VSAT (25W BUC), BW = 108MHz, Ka band (Antenna A 6G)
Max EIRP	49 dBW	49.4 dBW
G/T	11.2 dBi	11.6 dBi
Polarization	RHCP/LHCP	RHCP/LHCP

One Way Delay @ min elevation	142 ms	142 ms

Table 9 GEO conclusion

Satellite backhaul over a MEO@8000 km satellite:

Parameter	**5G time frame KPI Target**	**6G time frame KPI Target**
Peak data rate (user terminated or DL)	240 Mbps	740 Mbps
Peak data rate (user terminated or UL)	190 Mbps	440 Mbps
Experienced user throughput (user terminated or DL)	240 Mbps	740 Mbps
Experienced user throughput (user originated or UL)	190 Mbps	440 Mbps
Beam/cell capacity DL	1333 Mbps	1370 Mbps
Beam/cell capacity UL	1055 Mbps	814 Mbps
Total number of Beams/cells DL	16	100
Total number of Beams/cells UL	16	100
Minimum elevation angle	30°	30°
Acquisition time	60s	20s
UE type	VSAT (25 W BUC), BW = 36 MHz, Ka band (Antenna A)	VSAT (25 W BUC), BW = 108 MHz, Ka band (Antenna A 6G)
Max EIRP	49 dBW	49.4 dBW
G/T	11.2 dBi	11.6 dBi
Polarization	RHCP/LHCP	RHCP/LHCP
One Way Delay @ min elevation	37 ms	37 ms

Table 10 MEO conclusion

Satellite backhaul over a LEO@1200 km satellite

Parameter	**5G timeframe KPI Target**	**6G timeframe KPI Target**
Peak data rate (user terminated or DL)	210 Mbps	660 Mbps
Peak data rate (user terminated or UL)	210 Mbps	510 Mbps
Experienced user throughput (user terminated or DL)	210 Mbps	660 Mbps
Experienced user throughput (user originated or UL)	210 Mbps	510 Mbps
Beam/cell capacity DL	1167 Mbps	1222 Mbps
Beam/cell capacity UL	1167 Mbps	944 Mbps

Total number of Beams/cells DL	16	100
Total number of Beams/cells UL	16	100
Minimum elevation angle	30°	30°
Acquisition time	60s	30s
UE type	VSAT (25 W BUC), BW = 36 MHz, Ka band	VSAT (25 W BUC), BW = 108 MHz, Ka band
Max EIRP	49 dBW (Antenna A)	49.4 dBW (Antenna A 6G)
G/T	11.2 dBi	11.6 dBi
Polarization	RHCP/LHCP	RHCP/LHCP
One Way Delay @ min elevation	7 ms	7 ms

Table 11 LEO conclusion

4.2 Links to/from HAPS-UE

4.2.1 Link and use case description

This analysis focuses on a link between High Altitude Platform Station (HAPS) acting as a HAPS IMT base station (HIBS) flying in stratospheric altitude of FL600 (18.3 km) and terrestrial handset type of UE for both Uplink and Downlink data transmission, as depicted on the Figure 3. The analysis assumes Mobile Broadband type services such as web browsing, voice and messaging, OTT services, video streaming etc. Thus, we do not focus on IoT or fixed wireless access (FWA) use cases.

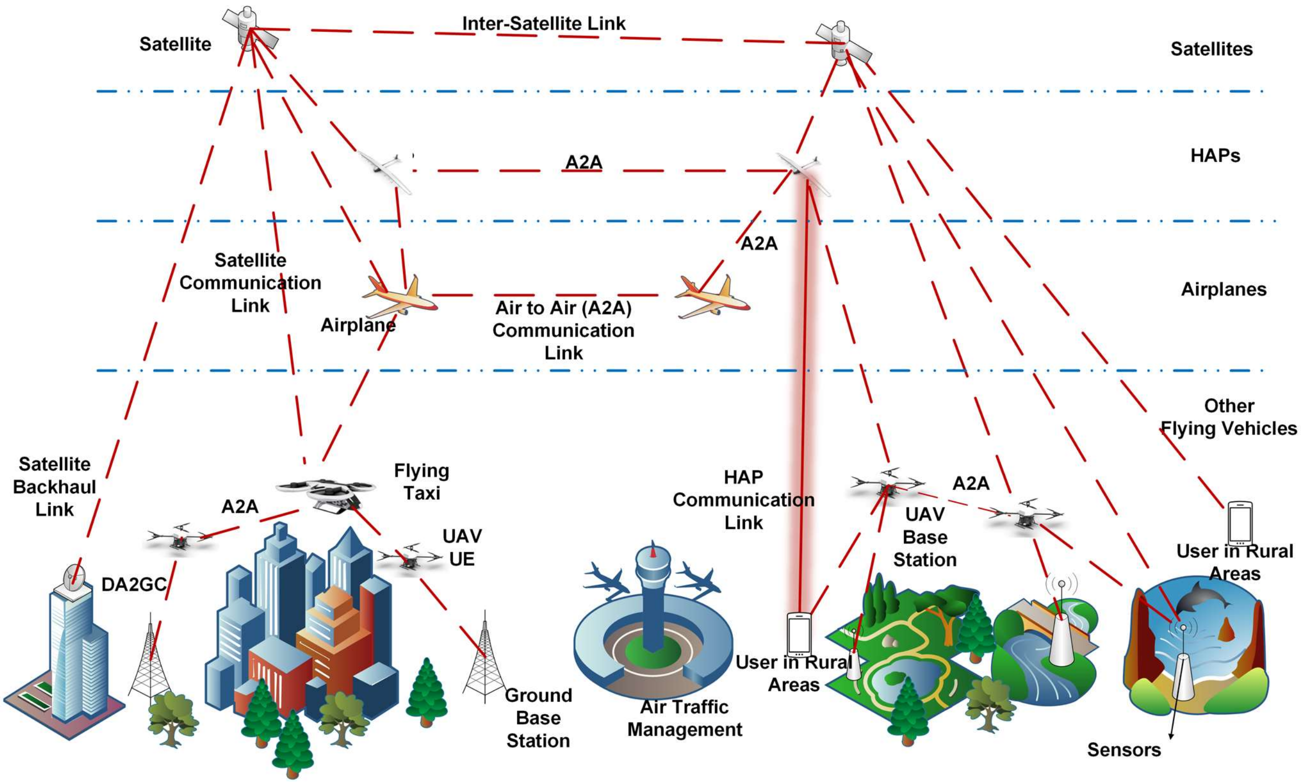

Figure 3 HAPS-UE link in 6G-Sky reference architecture

4.2.2 Description of key assumptions and system parameters

As a baseline for the analysis, we assume a 3GPP 5G (NR) RAT based link for the 5G timeframe scenario and have set a number of key assumptions and system parameters to represent future 6G timeframe scenario, as depicted in Table 12.

Parameter	**5G Timeframe**	**6G Timeframe**
Link Distance	18 km and 63 km	18 km and 63 km
Frequency Band	band n7 / 2.6 GHz	"FR3" 8 GHz

Channel Bandwidth	20 MHz	100 MHz
BS Total Tx power	43 dBm (20 W)	53 dBm (200 W)
UE Total Tx power	23 dBm (200 mW)	26 dBm (400 mW)
BS Antenna Bore-sight Gain	28.1 dBi	37.7 dBi
UE Antenna Bore-sight Gain	0 dBi	12.5 dBi
Interference Margin	3 dB	1 dB
Spectrum Efficiency Factor	1.0	1.2

Table 12 Key system parameter assumptions

With respect to the Link Distance we have analyzed two scenarios, 18 km for UE directly underneath the HAPS, so called nadir position, and 63 km for UE in cell service edge area which is assumed to be 50 km from cell center. The link geometries illustrating these scenarios are shown in Figure 4.

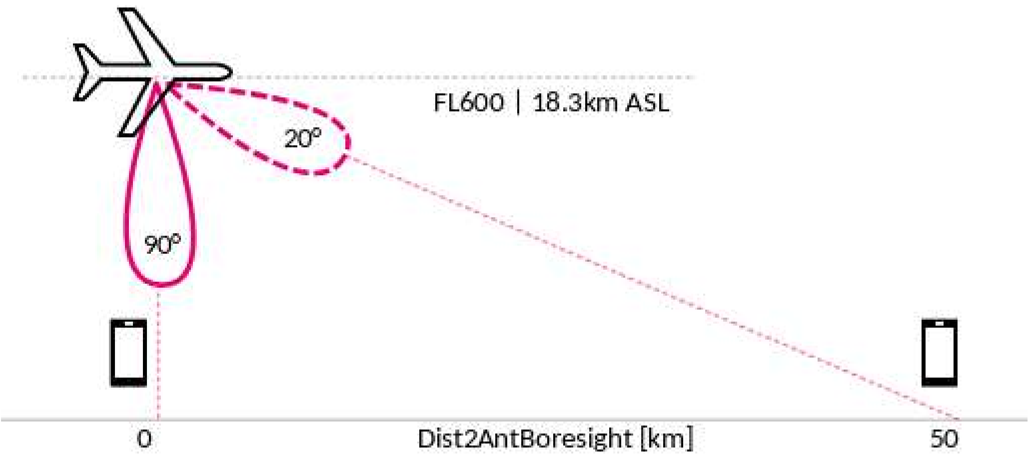

Figure 4 HAPS link geometry assumptions

For frequency bands, in 5G timeframe scenario we have used one of the bands that is approved for HIBS use case [15], specifically band n7 (2600 MHz). This is generally a suitable candidate for rural operations, since the band is predominantly used in urban areas and is generally under-utilized in rural areas. For 6G timeframe, we assume use of higher frequencies at 8 GHz in so called FR3 range (7-24 GHz), as this range is being studied for IMT use. Use of this range would possibly allow for higher overall bandwidth, however for the study we have assumed a rather conservative 100 MHz channel bandwidth.

For BS total Tx power, the 5G timeframe assumes a typical power of 20 W per Tx path available for macro-scale Radio Unit (RU). Going to 6G timeframe, we are aiming to use multi-beam active antenna to cover target area with multiple cells as illustrated in Figure 5, therefore we increased the aggregated output power to 200 W. From PA design perspective it would be possible to go even higher already today, however due to possibly limited energy budget for HAPS payload, we want to keep the active antenna's RF power and its power consumption at realistic level.

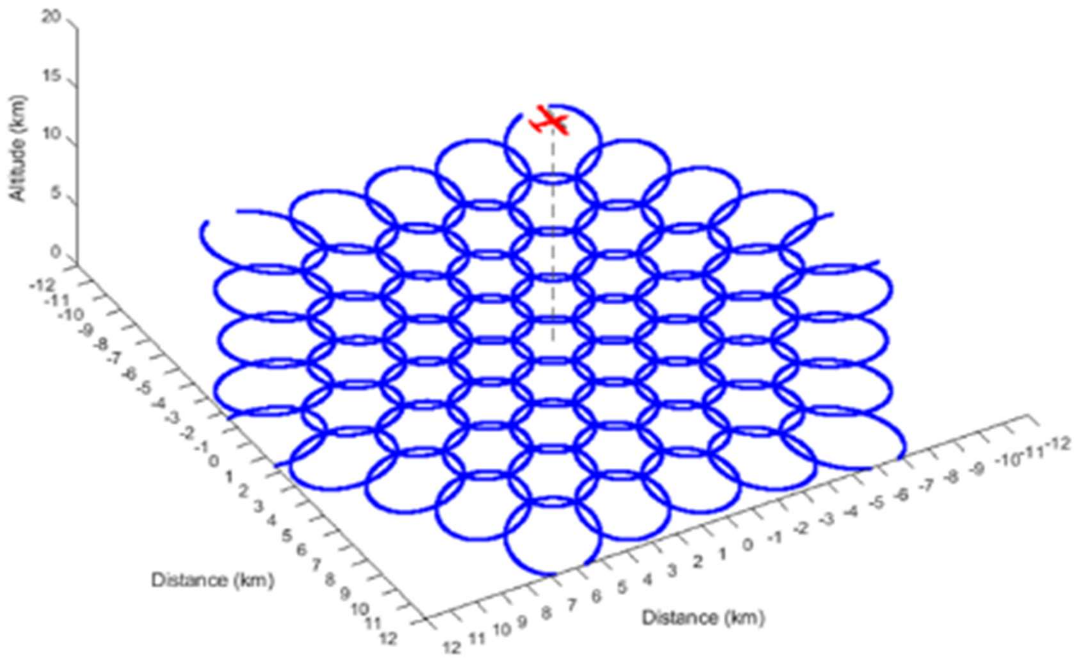

Figure 5 Example beam Layout for multi-beam antenna

From UE side we stay on conservative values for both 5G and 6G timeframe and assume only currently specified UE power classes 2 and 3, considering SAR limitations, battery life etc.

Main antenna characteristics assumed for the HAPS-UE link are detailed in Table 13. For BS side, to keep the antenna size reasonable, we assume rectangular shape with less than 1 m^2 surface area as depicted in Figure 6. For 6G timeframe, we assume the use of beamforming capable antenna also for the UE side, enabled by use of FR3 spectrum range.

Freq (GHz)	**Link Side**	**Architecture**	**Gain (dBi)**		**Min Size (mm)**
			Nadir (90°)	**20°**	
2.6	HAPS	16x16	28.1	23.4	865
8	HAPS	48x48	37.7	33	881
8	UE	4x4	12.5	9.1	56

Table 13 Antenna architecture assumptions

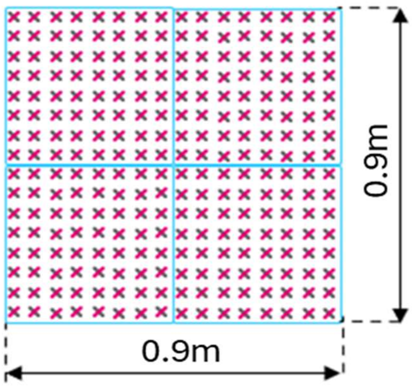

Figure 6 Physical layout example of 16x16 dual polarized antenna array for Band 7 (2600 MHz)

For 6G timeframe, we lower the Interference margin by 2 dB as we assume the use of high gain antennas with improved sidelobe suppression and advancements in interference cancellation methods. Also, we anticipate an improvement in Spectral Efficiency by a factor of 1.2, by use of higher modulation schemes, more efficient use of guard bands etc.

4.2.3 Link budget calculations

The link budget calculation focuses on two geometric scenarios, representing two different UE locations within the HIBS service area as depicted in Figure 4. These locations provide extreme cases with respect to the link distance, which is one of dominating factors in the link budget calculation.

Further, the calculation is done assuming different system parameters for 5G and 6G timeframes, as well as is separated for Downlink and Uplink analysis.

Since the link is considered to be of Line of Sight (LOS) type, we use simple a free space path loss model for attenuation calculation both for Downlink and Uplink.

Finally, for 6G timeframe, we use two key assumptions as improvement over 5G as described in chapter 4.2.2. First, we use lower interference margin resulting in higher SNR, and therefore higher achievable throughput, and additionally multiply it by spectrum efficiency factor of 1.2.

4.2.3.1 Downlink direction

Detailed link budget calculation for downlink direction (i.e. from the BS to the UE) is provided in Figure 7. A link to spreadsheet is provided in Annex 8.3.

HAPS - UE | Downlink			6G timeframe		5G timeframe	
			Scenario 1; HAPS Nadir position	Scenario 2; Service area edge position	Scenario 1; HAPS Nadir position	Scenario 2; Service area edge position
Freq	Link Budget Frequency	GHz	8.0	8.0	2.6	2.6
BW	Total Bandwidth	MHz	**100**	**100**	**20**	**20**
BSTxPwr	Total Transmit Power available per Transmit channel	W	**1.55**	**1.55**	**10**	**10**
BSTxPwr	Total Transmit Power available per Transmit channel	dBm	31.9	31.9	40.0	40.0
TxChanNo	Number of TX channels	-	**128**	**128**	**2**	**2**
DLLayers	Nunber of DL layers	-	**2**	**2**	**2**	**2**
BSTxPwrRE	TX power per Resource Element	dBm	17.9	17.9	12.0	12.0
LFeeder	Tx_FeederLoss (distribution loss)	dB	0.5	0.5	0.5	0.5
TxAntGain	Tx Antenna Gain	dBi	37.7	33.0	28.1	23.4
EIRPRE	**EIRP per RE**	**dBm**	**55.1**	**50.4**	**39.6**	**34.9**
EIRP	**Total EIRP**	**dBm**	**90.2**	**85.5**	**70.6**	**65.9**
Dist	Link Distance	km	18.3	63.0	18.3	63.0
FSPL	FSPL	dB	135.8	146.5	126.0	136.7
LAtmGas	Atmospheric Gases and Water Vapor Attenuation	dB	0.1	0.9	0.1	0.5
LRain	Rain Attenuation (ITU P.838-3, 10mm/h)	dB	0.1	2.6	0.1	0.2
Fading	Fading Margin	dB	10.0	10.0	10.0	10.0
PLTotal	**Path Loss Total**	**dB**	**146.0**	**159.9**	**136.2**	**147.4**
RxAntGain	Rx Antenna Gain	dBi	12.5	9.1	0	0
LBody	Body Loss	dB	3.0	3.0	3.0	3.0
RxDivGain	Receiver Diversity Gain	dB	3.0	3.0	3.0	3.0
RxLev	**RxLev at Receiver Input**	**dBm**	**-78.4**	**-100.5**	**-96.7**	**-112.5**
SCBW	Subcarrier BW (OFDM SCS)	kHz	30	30	15	15
SysTemp	System Temperature	K	290	290	290	290
RxNF	Rx LNA NF	dB	8	8	8	8
RxNfloor	Receiver Noise Floor	dBm	-121.2	-121.2	-124.2	-124.2
Interference	Interference Margin	dB	1.0	1.0	3.0	3.0
SEfactor	Spectrum efficiency increase factor	-	1.20	1.20	1.00	1.00
SNR	**SNR**	**dB**	41.8	19.7	24.6	8.7
Thput	**Throughput (5G NR based)**	**Mbps**	1251.0	813.5	161.0	74.6

Figure 7 HAPS-UE link budget for Downlink

Starting on BS (i.e. HIBS) side, we use OFDM based 5G NR system as a baseline. Thus, for further calculations, we need to first calculate the transmit power per Resource Element (RE) as shown in Figure 8.

SCS	Subcarrier Spacing	15	kHz		
TxChanNo	Number of TX channels	2	-	3.0	dB
BSTxPwr	Total Transmit Power available per Transmit channel	10	W	40.0	dBm
BSTxPwrTot	Total Transmit Power	20	W	43.0	dBm
BW	Total Bandwidth	20	MHz	106	RBs
REnum	RE number [RBnum*12]	1272	-	31.0	
CRP	Cell reference power	0.0079	W	9.0	dBm
BSTxPwrRE	**TX power per Resource Element**	**0.016**	**W**	**12.0**	**dBm**

Figure 8 Example calculation of RE power

Then we calculate the Total Effective Isotropic Radiated Power (EIRP) per RE.

$$EIRPRE\ (dBm) \ = \ BSTxPwrRE - LFeeder + TxAntGain$$

Total link loss between the transmitter and receiver pair consists of free space path loss, atmospheric effects and a margin for fading.

$$PLTotal\ (dB) = \ FSPL + LAtmGas + LRain + Fading$$

We then calculate received power level at receiver input per RE (effectively RSRP). For this we consider UE antenna gain, margin for body loss and Rx diversity gain.

$$RxLev\ (dBm) \ = \ EIRPRE - PLTotal \ + RXAntGain - LBody + RxDivGain$$

Ultimately, the link performance is dictated by the achieved Signal to Noise Ratio, which is impacted by the receiver implementation such as bandwidth, noise figure etc.

$$SNR \ = \ RxLev - RxNfloor - Interference$$

where the receiver noise floor is given by thermal noise and receiver noise figure.

$$RxNfloor = \ 10 * Log(k * T * B) + RxNF$$

The last step is to calculate the maximum achievable throughput for the given SNR. For this we apply the calculation method described in 3GPP TS 38.214, Section 5.1.3.2. As inputs for calculation, we use the following parameters:

- Modulation and Coding Scheme (MCS) Index
- Code Rate (R)
- Modulation Order (Q_m)
- Number of allocated Resource Blocks (RB)
- Number of Layers

From stratospheric flight experiments with 5G NR payload we get a mapping table between Synchronization Signal SINR (SS-SINR) and DL MCS as depicted in Figure 9, which we used to transform the calculated SNR from previous step to the MCS index (I_{MCS}).

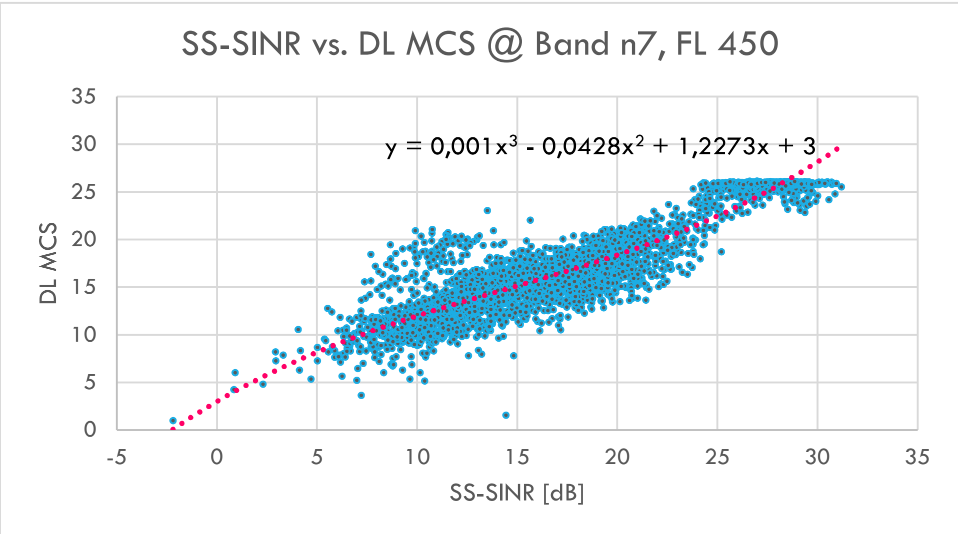

Figure 9 SS-SINR vs DL MCS

Based on *Table 5.1.3.1-2: MCS index table 2 for PDSCH* in 3GPP TS 38.214 we derive the Q_m and R values. With these values, we calculate the maximum Transport Block Size using cell bandwidth, number of layers and number of scheduled PDSCH symbols. Finally, we get the achievable throughput by multiplying the TBS with available slots.

4.2.3.2 Uplink direction

Detailed link budget calculation for uplink direction (i.e. from the UE to the BS) is provided in Figure 10. A link to spreadsheet is provided in Annex 8.3.

HAPS - UE | Uplink			6G timeframe		5G timeframe	
			Scenario 1; HAPS Nadir position	Scenario 2; Service area edge position	Scenario 1; HAPS Nadir position	Scenario 2; Service area edge position
Freq	Link Budget Frequency	GHz	8.0	8.0	2.6	2.6
BW	Total Bandwidth	MHz	**100**	**100**	**20**	**20**
UETxPwr	Total Tx Power available per TX channel	dBm	26.0	26.0	23.0	23.0
TxChanNo	Number of TX channels	-	**1**	**1**	**1**	**1**
ULLayers	Nunber of UL layers	-	**1**	**1**	**1**	**1**
TxAntGain	Tx Antenna Gain	dBi	12.5	9.1	0.0	0.0
LBody	Body loss	dB	3.0	3.0	3.0	3.0
EIRP	**Total EIRP**	**dBm**	**35.5**	**32.1**	**20.0**	**20.0**
Dist	Link Distance	km	18.3	63.0	18.3	63.0
FSPL	FSPL	dB	135.8	146.5	126.0	136.7
LAtmGas	Atmospheric Gases and Water Vapor Attenuation	dB	0.2	0.9	0.1	0.5
LRain	Rain Attenuation (ITU P.838-3, 10mm/h)	dB	1.6	2.6	0.1	0.2
Fading	Fading Margin	dB	10.0	10.0	10.0	10.0
Interference	Interference Margin		1.0	1.0	3.0	3.0
PLTotal	**Path Loss Total**	**dB**	**148.6**	**160.9**	**139.2**	**150.4**
RxAntGain	Rx Antenna Gain	dBi	37.7	33.0	28.1	23.4
LFeeder	Rx Feeder Loss (distribution loss)	dB	0.5	0.5	0.5	0.5
RxDivGain	Rx Diversity Gain	dB	5.0	5.0	5.0	5.0
SEfactor	Spectrum efficiency increase factor	-	1.20	1.20	1.00	1.00
RxLev	**RxLev at Receiver Input**	**dBm**	**-70.9**	**-91.3**	**-86.6**	**-102.5**
CL	**Coupling Loss**	**dB**	**97**	**117**	**110**	**125.5**
BW	Total Bandwidth	MHz	100	100	20	20
SysTemp	System Temperature	K	290	290	290	290
RxNF	Rx LNA NF	dB	4	4	4	4
RxNfloor	Receiver Noise Floor	dBm	-90.0	-90.0	-97.0	-97.0
SNR	**SNR**	**dB**	**19.0**	**-1.4**	**10.3**	**-5.5**
Thput	**Throughput based on CL** (5G NR FDD n1 1T4R 20MHz)	**Mbps**	N/A	N/A	**52.1**	**11.6**
Thput	**Throughput based on SNR** (5G NR FDD n1 1T4R 20MHz)	**Mbps**	N/A	N/A	**57.4**	**14.6**
Thput	**Throughput based on CL** (5G NR TDD n78 1T8R 90MHz)	**Mbps**	**315.1**	**29.8**	N/A	N/A
Thput	**Throughput based on SNR** (5G NR TDD n78 1T8R 90MHz)	**Mbps**	**325.4**	**44.1**	N/A	N/A

Figure 10 HAPS-UE link budget for Uplink

As for the Downlink, we use OFDM based 5G NR system as a baseline for the Uplink, however calculation steps are slightly different. First, the total UE EIRP is calculated.

$$EIRP = UETxPwr + 10 * Log(TxChanNo) + TxAntGain - LBody$$

Total link loss between the transmitter and receiver pair consists of free space path loss, atmospheric effects and a margin for fading as well as interference margin.

$$PLTotal\ (dB) = FSPL + LAtmGas + LRain + Fading + Interference$$

We then calculate received power level at receiver input. For this we consider BS antenna gain, margin for feeder loss and Rx diversity gain.

$$RxLev\ (dBm) = EIRP - PLTotal + RXAntGain - LFeeder + RxDivGain$$

We derive the 5G timeframe throughput values using two different approaches:

a) Based on Coupling Loss (CL), calculated by:

$$CL = EIRP - RXLev$$

b) Based on Uplink SNR estimation:

$$SNR = RXLev - RxNFloor$$

where the receiver noise floor is given by thermal noise and receiver noise figure.

$$RxNfloor = 10 * Log(k * T * B) + RxNF$$

For throughput estimation, two different sets of log files from field experiments are used for mapping between CL and SNR to UL throughput. For 5G timeframe, data is based on Band n7 (2600 MHz) with 20 MHz channel bandwidth and 1T4R antenna configuration, and for 6G timeframe we use Band n78 (3600 MHz), 90 MHz channel bandwidth and 1T8R antenna configuration.

Data for band n78 is based on TDD system on 90 MHz bandwidth, while the target system is assumed to be FDD with 100 MHz bandwidth. Thus, we normalize the measured data to the target system. This results to CL and SNR vs Throughput graphs as shown in Figure 11 and Figure 12.

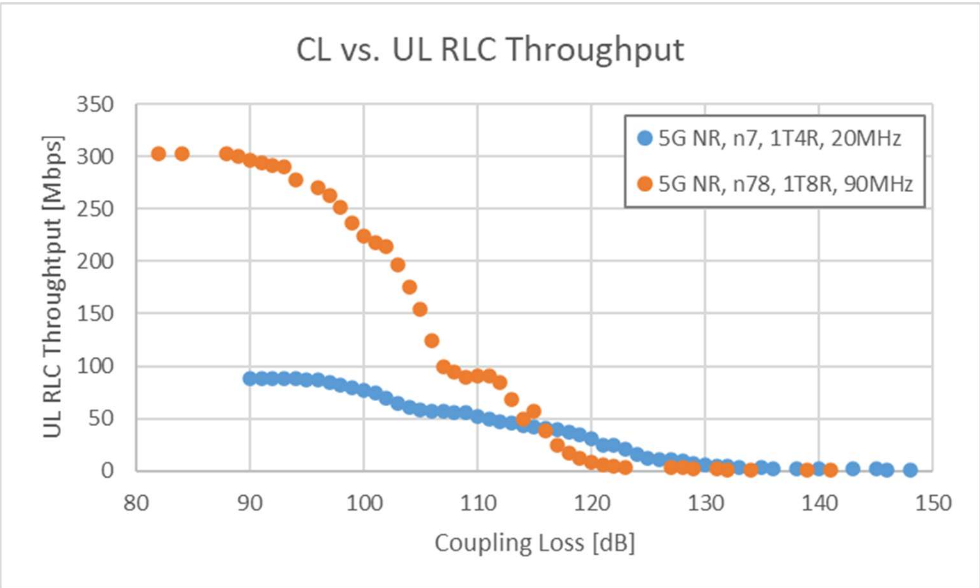

Figure 11 Coupling Loss vs Throughput

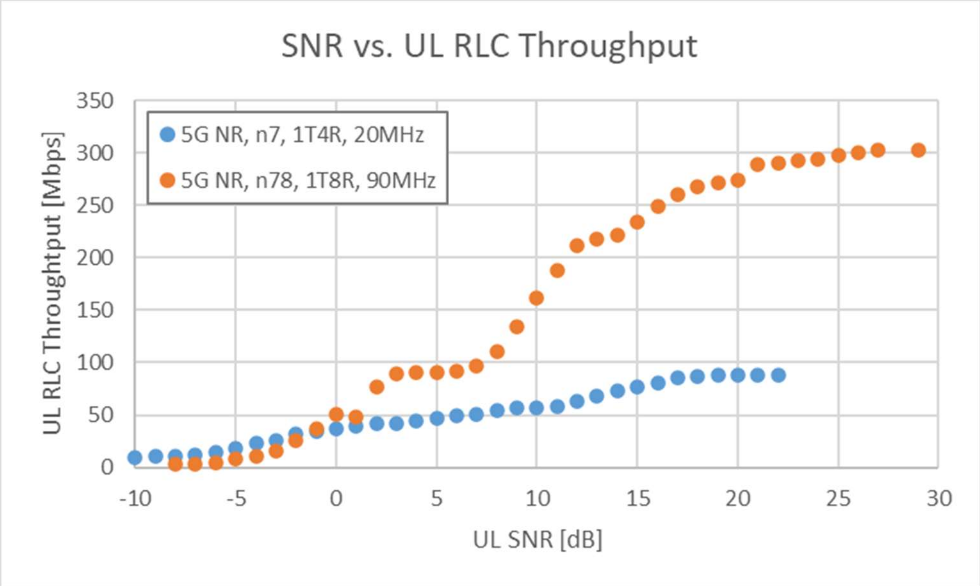

Figure 12 SNR vs Throughput

4.2.4 Comparison with target KPIs and conclusion

Comparing with the 6G target KPIs outlined in chapter 3, we can conclude that the throughput values for the Downlink resulting from the above link budget study meet the target values as shown in Table 14.

For Uplink throughput calculation, two different methods were used, resulting in slightly different values. The Table 14 shows averaged value of both methods.

KPI Targets for 6G timeframe	Peak Data Rate	Experienced Data Rate
Data rate (user terminated or DL)	1000 Mbps	500 Mbps
Data rate (user originated or UL)	100 Mbps	50 Mbps

Derived throughput values for 6G	Peak Data Rate	Cell Edge Data Rate
Data rate (user terminated or DL)	1250 Mbps	810 Mbps
Data rate (user originated or UL)	320 Mbps	37 Mbps

Table 14 Target and calculated throughput values

4.3 Links to terrestrial BS

4.3.1 Links from terrestrial base stations to airborne users

This section presents a link-level analysis of terrestrial mobile networks serving aerial users flying below 2000 m height (i.e., up to approximately 6500 ft). The focus is on the data channel for uplink (UL) and downlink (DL), with the DL being the link from a base station transmitting data to an aerial user, and the UL being the link from an aerial user transmitting to a terrestrial base station. This link is highlighted in red in Figure 13.

The link performance analysis is applicable to airborne vehicles such as uncrewed aerial vehicles (UAV), electric vertical take-off and landing (eVTOL) aircraft, and helicopters.

Frequencies within FR1 and FR3 are considered.

4.3.2 Assumption on system, network and base station parameters

System parameters are listed in Table 15.

Parameter	5G timeframe	6G timeframe
Carrier frequency (GHz)	3.5	10
Bandwidth (MHz)	20	100
Sub carrier spacing (kHz)	30	30
Base station transmit power (dBm)	53	53
Base station antenna gain (dBi)	24.2	33.8

Table 15 System parameters for links to/from terrestrial base station

Terrestrial base stations for the 5G timeframe are equipped with a 4-by-8 array of subarrays where each subarray has 2-by-1 cross-polarized antennas. For 6G timeframe, base station antennas consist of a configuration of a 4-by-24 array of subarrays and each subarray has 6-by-1 cross-polarized antennas. The antenna elements have 65° half-power beamwidth in both azimuth and elevation, and an element gain of 6.2 dBi.

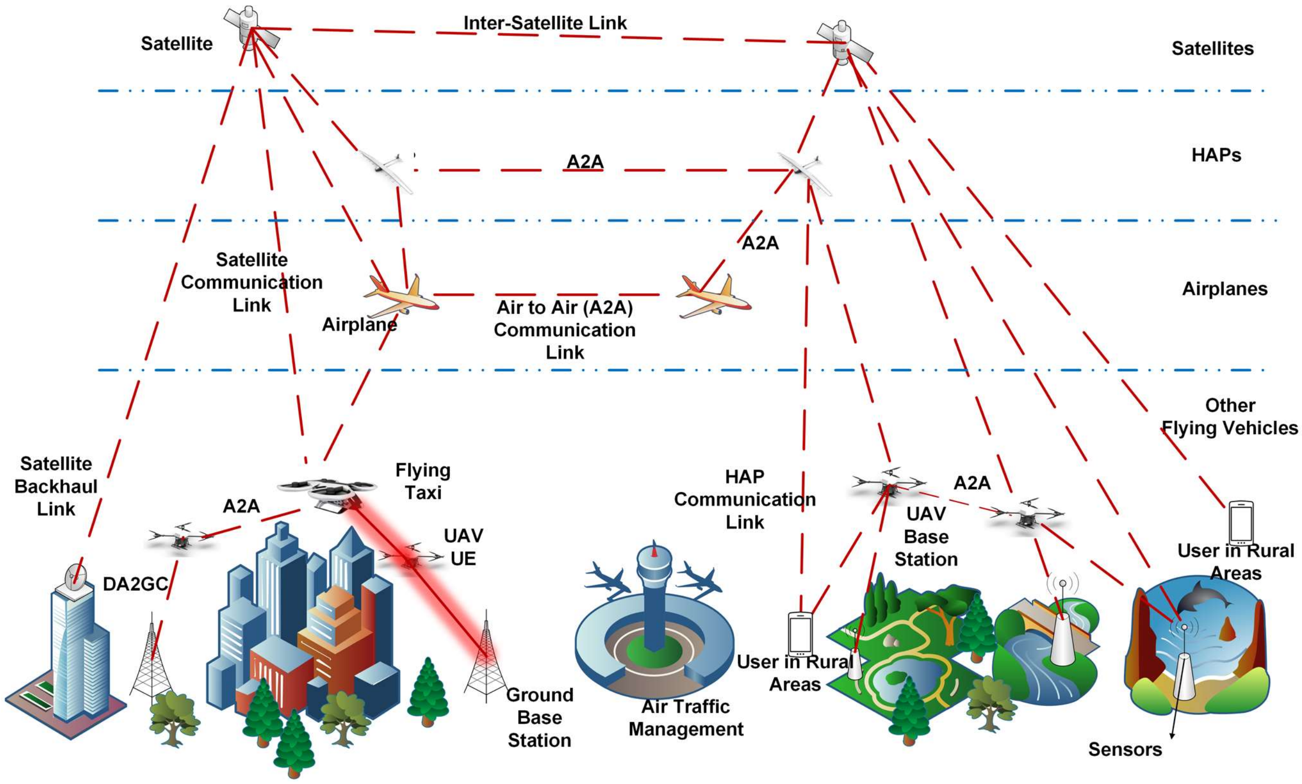

Figure 13 Terrestrial base station to low-flying airborne UE link (highlighted) within 3D Network Architecture

4.3.3 Description of assumptions on aerial user's equipment

This analysis considers terrestrial networks serving aerial UEs. Two types of airborne vehicles are considered, UAVs and eVTOL vehicles. UAVs are assumed to operate at flying heights of up to 300 m (≈1000 ft). To cater for Urban Air Mobility (UAM) use cases beyond UAVs, flying heights of up to 1000 m are studied for UAM vehicles such as eVTOL. Analysis of flying heights between 1000 m and 2000 m expected for other Advanced Air Mobility (AAM) use cases is not included in the current analysis to keep the focus on promising use cases, however extension of the current analysis to those flying heights is straight forward. Assumptions on flying heights of airborne vehicles considered in the current analysis are illustrated in Figure 14.

For UAM, using either eVTOL or helicopters, typical flying heights are expected to be up to 1000 m. For these aerial vehicles, flying at heights higher than 3000 m (≈10 000 feet) becomes challenging due to cabin pressurization requirements. For example, European Union Aviation Safety Agency (EASA) requires the use of supplemental oxygen masks when the cabin altitude exceeds 10 000 feet for more than 30 minutes.

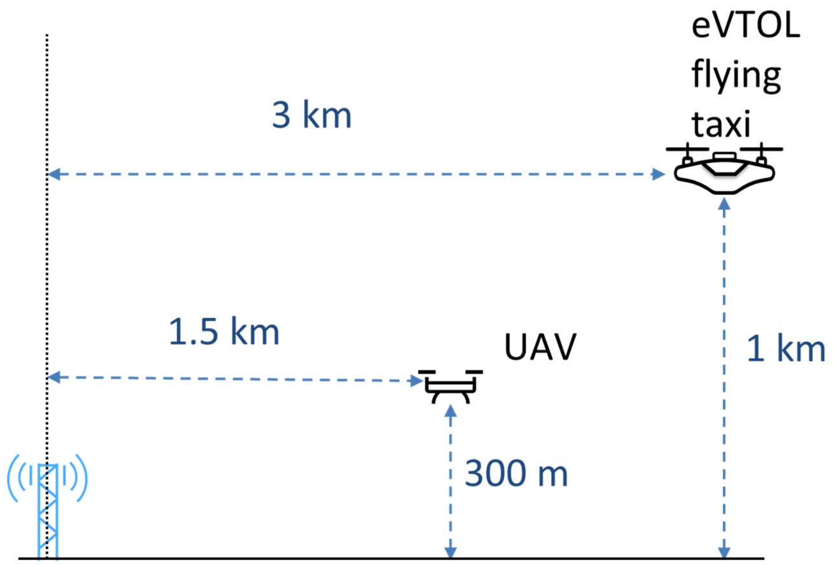

Figure 14 Assumptions on airborne vehicles

4.3.4 Link budget calculations

Link budget for UAV case is calculated for both the 5G and 6G timeframe, while the link budget for the flying taxis is computed for 6G timeframe. Table 16 shows link budget in the downlink for the relevant scenarios:

Parameter	**Symbol**	**Unit**	TN to UAV (DL) 5G	TN to UAV (DL) 6G	TN to Flying taxi (DL) 6G
System parameters:					
Carrier frequency	Freq	GHz	3.5	10	10
Channel Bandwidth	BW	MHz	20.0	100.0	100.0
Transmitter side:					
Transmit power	P_out	dBm	49.0	53.0	53.0
Antenna Gain	G_TX	dBi	24.2	33.8	33.8
Cable loss, line losses, and switch losses	L_implementationTX	dB	2.0	2.0	2.0
Pointing losses	L_pointingTX	dB	1.0	3.0	2.0
Path:					
Total TX to RX distance		m	1525.0	1525.0	3154.5
Path loss	PL	dB	110.0	119.1	125.4
Metrics:					

Effective Isotropically Radiated Power	EIRP	dBm	70.2	81.8	82.8
Signal-to-noise ratio	SNR	dB	52.2	42.1	36.2
Signal-to-Interference-plus-noise ratio	SINR	dB	46.1	36.1	30.2
Capacity	C	Mbps	281.4	1179.6	986.4
Throughput	Thput	Mbps	109.8	587.7	587.7

Table 16 Base station – airborne UE link budget in DL

For the UL, Table 17 shows the uplink link budget for the 5G and 6G timeframes.

Parameter	**Symbol**	**Unit**	UAV to TN (UL) 5G	UAV to TN (UL) 6G	Flying taxi to TN (UL) 6G
System parameters:					
Carrier frequency	Freq	GHz	3.5	10	10
Channel Bandwidth	BW	MHz	20.0	100.0	100.0
Transmitter side:					
Transmit power	P_out	dBm	23.0	23.0	26.0
Pointing losses	L_pointingTX	dB	1.0	3.0	2.0
Path:					
Total TX to RX distance		m	1525.0	1525.0	3154.5
Path loss	PL	dB	110.0	119.1	125.4
Receiver side:					
Antenna Gain	G_RX	dBi	24.2	33.8	33.8
Metrics:					
Received signal power	S_RX	dBm	-66.2	-68.9	-71.8
Signal-to-noise ratio	SNR	dB	30.2	18.1	15.2
Signal-to-Interference-plus-noise ratio	SINR	dB	26.1	14.1	11.2
Capacity	C	Mbps	159.5	466.8	376.4
Throughput	Thput	Mbps	53.7	186.7	150.6

Table 17 Base station – airborne UE link budget in UL

In Table 16 and Table 17, throughput is computed using the following approximation described in section 6.2.9 in [6]

$$Thput(SINR) = \begin{cases} 0 & for\ SINR < SINR_{Min} \\ \alpha\ log_2(1 + SINR) & for\ SINR_{Min} \le SINR < SINR_{Max} \\ \alpha\ log_2(1 + SINR_{Max}) & for\ SINR \ge SINR_{Max} \end{cases}$$

Where $SINR_{Min}$ is the minimum SINR of the code set used in link adaptation, $SINR_{Max}$ is the maximum SINR of the code set, and α is an attenuation factor representing implementation losses. We consider a TDD configuration with DL:UL ratio of 3:2.

Throughput values presented in Table 16 and Table 17 show that target values for 6G time frame presented in section 3 are met.

More details on the calculation can be found in Annex 8.4.

4.3.5 Related work within the 6G-Sky project

Several studies related to the link between ground base station and aerial UEs have been performed within the context of 6G-Sky. For example, in the context of ground base station antenna design, [7] proposes antenna solution for direct-air-to-ground communications, with an antenna design for the 5.9-8.5 GHz band. The main advantages of the solution include wide-band, high-isolation antenna array concept for the ground BS antenna.

High mobility of airborne vehicles introduces challenges related to channel aging, with short-time channel coherence. In this aspect, [8] introduces a novel minimum mean square error (MMSE) receiver that depends only on CSI error statistics and the channel's correlation coefficient. The proposed receiver outperforms other state-of-art methods, especially those with higher autoregressive coefficients. The paper [9] focuses on the impact of pilot spacing in the uplink MU-MIMO systems operating in aging channels. It provides analytical expression between pilot spacing and achieved uplink spectral efficiency for MIMO systems as a function of the path loss, Rician factor and Doppler frequency. The paper also proposes a procedure to determine near-optimal pilot spacing that ensures high quality channel estimates, good link quality and high spectral efficiency in the uplink of terrestrial MIMO systems serving UAVs.

Cell-free systems are expected to play an important role in next generation mobile networks. The work in [10] explores cell-free massive MIMO systems focusing on uplink power allocation. Using a game theory framework, the paper proposes distributed power control approach that enhances energy utilization in user terminals and strikes a balance between spectral and energy efficiency. Antenna tilting can also impact the performance of cell-free systems, this is investigated in [11] for the case when the system serves both ground UEs and UAVs. The research shows that, while uptilt angles benefit UAVs, a fixed downward tilt with linear array setup is best for the entire system. This is due to the loss in spectral efficiency of UAVs is not as significant compared with ground UEs, because UAVs already have good rates and higher spectral efficiency than ground UEs. The work of [12] addresses the challenging problem of jointly controlling pilot-and-data power in cell-free systems. The study formulates two optimization objectives, maximizing minimum spectral efficiency and total spectral efficiency. A solution based on deep reinforcement learning is proposed that outperforms benchmarking algorithms in terms of minimum spectral efficiency and sum spectral efficiency for several scenarios.

In 5G New Radio (NR), multi-antenna technologies such as massive MIMO and beamforming are beneficial for dual-use networks, i.e., networks serving both terrestrial and aerial users. This is studied in [14] on 3GPP compliant technologies, and four main conclusions are obtained. A first conclusion is that dual-use cellular networks using UE-specific beamforming methods outperform networks using cell-specific beamforming even when uptilted antennas are used. A second conclusion is that the spatial diversity increases when there are aerial users in the system, and this can be used by MU-MIMO to co-schedule more users on the same time-frequency resource. A third conclusion is that significant interference reduction, in both uplink and downlink, is achieved when aerial UEs are equipped with directional antennas. Finally, the paper points out that one of the key challenges to realize advanced beamforming techniques for Advanced Air Mobility is the proper acquisition of CSI at the transmitter side, especially in high mobility scenarios.

A networks perspective of the performance of dual-use network is presented in [13]. The focus is on the coupling between interference and the network load when using technologies such as MU-MIMO, aerial-specific power control and AUE directional antennas. The results show that technologies providing both a reduction in interference and an improved SINR can help dual-use networks to keep appropriate QoS while maintaining a low system-wise resource utilization. For example, managing aerial UE (AUE) interference by using AUE-specific power control is beneficial in many scenarios, but when combined with other interference reduction technologies such as AUE directional antennas the benefits of AUE-specific power control can be limited or non-existent.

4.4 Feeder links to satellite

4.4.1 Assumptions on system parameters

The limitations in the design of the feeder links are the PFD limits for the downlink, specified by the ITU and the available bandwidths in different frequency ranges.

At this point it should be mentioned that the ITU-R only makes recommendations for the respective regions regarding the limits and that national agencies can also change these for their countries, but we take the ITU's specifications in our considerations into account.

In addition to the regulatory requirements, the following assumptions were made for the specification of the feeder links:

- As described in [23] the 5G NR waveform CP-OFDM suffer significant performance degradation for downlink compared to DVB-S2X due to higher peak-to-average power ratio (PAPR) at higher order modulation. For that reason, we assume 5G NR for the case, if the satellite payload is transparent. For regenerative payloads 5G NR or DVB-S2X could be used in general. As a simplification, since it is not specified how the processing payload is implemented on the UE side (HAPS, UAV, flying taxis) from the satellite perspective, the data rate calculation is based on 5G NR, even if DVB-S2X is slightly more efficient for feeder links.
- Waveform for the 6G timeframe is the same as for 5G (CP-OFDM).
- At the current stage, the FR2-NTN includes only the frequency band Ka (17.3 GHz to 30.0 GHz), but for the terrestrial applications the FR2 includes also frequencies up to 71 GHz (also

the Q/V band). For that reason, we consider Q/V band and especially the higher BW available in Q/V band for the 6G timeframe.

Parameter	**5G Timeframe**	**6G Timeframe**
Link Distance	38178 km (35786 km altitude and an elevation angle of 35°)	
Frequency Band	FR2 NTN (Ka band)	FR2 (Q/V band)
Channel Bandwidth	29.5 – 30 GHz (UL): 500 MHz 28.6 – 29.1 GHz (UL): 500 MHz 19.7 – 20.2 GHz (DL): 500 MHz 18.3 – 19.3 GHz (DL): 1 GHz [16]	42.5 – 43.5 GHz (UL): 1 GHz 47.2 – 50.2 GHz (UL): 3 GHz 50.4 – 51.4 GHz (UL): 1 GHz 37.5 – 39.5 GHz (DL): 2 GHz 40.5 – 42.5 GHz (DL): 2 GHz [17]
GW EIRP	+85 dBW	+95 dBW
GW G/T	43.7 dB/K [21]	42.8 dB/K [18]
Satellite EIRPD	57.6 dBW/MHz[2]	57.6 dBW/MHz
Satellite G/T	29.1 dB/K [22]	33.9 dB/K [22]
Atmospheric loss[3]	UL: 4.3 dB DL: 2.2 dB	UL: 9.8 dB DL: 6.9 dB
Additional losses	3 dB	3 dB

Table 18 System parameters for links to/from ground station to GEO satellite

In the 6G timeframe, LEO satellite altitude could be lower than for the 5G timeframe to achieve a better link budget also to smaller UE (direct-to-device). Whether it is financially viable to implement a LEO constellation at an altitude of for example 400 km (significantly more satellites are required to achieve coverage in a certain area of the earth than with an LEO 600 constellation) or to ensure coverage with HAPS if necessary, is not considered here. A LEO constellation at an altitude of 600 km is therefore assumed for both 5G and 6G timeframes.

Parameter	**5G Timeframe**	**6G Timeframe**
Link Distance	1075 km for LEO at 600 km altitude and an elevation angle of 30°	1075 km for LEO at 600 km altitude and an elevation angle of 30°
Frequency Band	FR2 NTN (Ka band)	FR2 (Q/V band)
Channel Bandwidth	29.5 – 30.0 GHz (UL): 500 MHz 28.6 – 29.1 GHz (UL): 500 MHz 19.7 – 20.2 GHz (DL): 500 MHz 18.3 – 19.3 GHz (DL): 1 GHz [16]	42.5 – 43.5 GHz (UL): 1 GHz 47.2 – 50.2 GHz (UL): 3 GHz 37.5 – 39.5 GHz (DL): 2 GHz 40.5 – 42.5 GHz (DL): 2 GHz [17]
GW EIRP	+80 dBW	+81 dBW [19]
GW G/T	40.0 dB/K [20]	35.1dB/K [19]
Satellite EIRPD	26.6 dBW/MHz[4]	26.6 dBW/MHz

[2] ITU-R Radio Regulations, Edition of 2020, http://handle.itu.int/11.1002/pub/814b0c44-en: Defined PFD Limit in dB(W/m2) for angles of arrival (25°-90°) above the horizontal plane with Reference bandwidth of 1MHz

[3] ITU-R P.618

[4] ITU-R Radio Regulations, Edition of 2020, http://handle.itu.int/11.1002/pub/814b0c44-en: Defined PFD Limit in dB(W/m2) for angles of arrival (25°-90°) above the horizontal plane with Reference bandwidth of 1MHz

Satellite G/T	9.1 dB/K [22]	13.3 dB/K [22]
Atmospheric loss[5]	UL: 4.8 dB DL: 2.5 dB	UL: 10.9 dB DL: 7.7 dB
Additional losses	3 dB	3 dB

Table 19 System parameters for links to/from ground station to LEO satellite

4.4.2 Link budget calculations

4.4.2.1 5G timeframe - Ground station to GEO

The figure below shows the uplink link budget calculation for a max. available BW of 400 MHz and a max. resulting data rate of 2.5 Gbit/s.

Uplink - FR2: GEO 35786 km, elevation angle 35°																	
UE		Satellite										Results - 5G NR Performance					
max. EIRP [dBW]	max. EIRP Density [dBW/MHz]	Antenna Gain [dBi]	G/T [dB/K]	Altitude [km]	Frequency [MHz]	max. available BW [MHz]	FR	SCS [kHz]	N_{RB}	Elevation angle [°]	Slant range [km]	CNR [dB]	max. eff. BW [MHz]	eff. BW [MHz]	Count of RB with a BW of 1,44 MHz	Spectral Efficiency [Bit/s/Hz]	max. Datarate [Mbit/s]
85,00	59,2	54,9	29,1	35786	29000,0	400	2	120	264	35	38178	36,3	380,16	380,16	264	6,67	2534,60

Figure 15 Uplink (ground station to GEO) link budget for 5G timeframe

The achievable data rates for further bandwidths as defined in 3GPP TS 38.101 are shown in Table 8. As the CNR is high enough, the increase of the bandwidth leads to an increase in data rate without a sufficient reduction of the spectral efficiency.

max. available BW [MHz]	**max. data rate [Mbit/s]**	**Data rate/BW factor**
100	633.65	6.34
200	1267.3	6.34
400	2534.6	6.34
800	4761.98	5.95
1600	9523.96	5.95
2000	11367.31	5.68

Table 20 Data rates from ground station to GEO satellite for different BW and the resulting data rate to BW factor

As the maximum bandwidth in the Ka band is 500 MHz, it makes sense to select the specified 3GPP bandwidth of 400 MHz. The total data rate of the feeder links can be increased if several links are set up in parallel and the frequency reuse factor of 2 (RHCP and LHCP) is used.

The link budget results for the DL are shown below.

[5] ITU-R P.618

Downlink - FR2: GEO 35786 km, elevation angle 35°															
Satellite			UE									Results			
PFD [dBW/m²]	Altitude [km]	max. EIRP Density [dBW/MHz]	Antenna Gain [dBi]	G/T [dB/K]	Frequency [MHz]	max. BW [MHz]	FR	SCS [kHz]	N_{RB}	Elevation angle [°]	Slant rage [km]	CNR [dB]	max. eff. BW [MHz]	Spectral Efficiency - 5G NTN [Bit/s/Hz]	max. Datarate - 5G NTN [Mbit/s]
-105,0	35786	57,6	68,0	43,7	19000,0	100,0	2	120	66	35	38178	52,0	95,04	6,07	577,3
-105,0	35786	57,6	68,0	43,7	19000,0	200,0	2	120	132	35	38178	52,0	190,08	6,07	1154,7
-105,0	35786	57,6	68,0	43,7	19000,0	400,0	2	120	264	35	38178	52,0	380,16	6,07	2309,3
-105,0	35786	57,6	68,0	43,7	19000,0	800,0	2	480	124	35	38178	52,0	714,24	6,07	4338,7
-105,0	35786	57,6	68,0	43,7	19000,0	1600,0	2	480	248	35	38178	52,0	1428,48	6,07	8677,4
-105,0	35786	57,6	68,0	43,7	19000,0	2000,0	2	960	148	35	38178	52,0	1704,96	6,07	10356,9

Figure 16 Downlink (GEO to ground station) link budget for 5G timeframe

The results of the link budget calculation show that a high CNR can be achieved and thus the transmission can take place with the highest Modulation and Coding Scheme (MCS) of 5G. Since no increase in spectral efficiency can be achieved above a CNR of 34.7 dB, it is recommended to reduce the transmission power of the satellite and thus the PFD.

4.4.2.2 6G timeframe - Ground station to GEO

As already described in the assumptions, the Q/V band is used for the feeder links in the 6G timeframe. This means that the maximum bandwidth specified in 3GPP - 2 GHz - can be used. The higher atmospheric losses have no influence on the maximum spectral efficiency, as the link margin is very high.

Uplink - FR2: GEO 35786 km, elevation angle 35°																	
UE		Satellite										Results - 5G NR Performance					
max. EIRP [dBW]	max. EIRP Density [dBW/MHz]	Antenna Gain [dBi]	G/T [dB/K]	Altitude [km]	Frequency [MHz]	max. available BW [MHz]	FR	SCS [kHz]	N_{RB}	Elevation angle [°]	Slant range [km]	CNR [dB]	max. eff. BW [MHz]	eff. BW [MHz]	Count of RB with a BW of 11,52 MHz	Spectral Efficiency [Bit/s/Hz]	max. Datarate [Mbit/s]
95,00	62,7	59,7	33,9	35786	47000,0	2000	2	960	148	35	38178	34,9	1704,96	1704,96	148	6,67	11367,31

Figure 17 Uplink (ground station to GEO) link budget for 6G timeframe

The highest spectral efficiency is also achieved in the downlink, so that the 2 GHz bandwidth can also be used for the feeder link.

Downlink - FR2: GEO 35786 km, elevation angle 35°															
Satellite			UE									Results			
PFD [dBW/m²]	Altitude [km]	max. EIRP Density [dBW/MHz]	Antenna Gain [dBi]	G/T [dB/K]	Frequency [MHz]	max. BW [MHz]	FR	SCS [kHz]	N_{RB}	Elevation angle [°]	Slant rage [km]	CNR [dB]	max. eff. BW [MHz]	Spectral Efficiency - 5G NTN [Bit/s/Hz]	max. Datarate - 5G NTN [Mbit/s]
-105,0	35786	57,6	68,0	43,7	39000,0	100,0	2	120	66	35	38178	41,1	95,04	6,07	577,3
-105,0	35786	57,6	68,0	43,7	39000,0	200,0	2	120	132	35	38178	41,1	190,08	6,07	1154,7
-105,0	35786	57,6	68,0	43,7	39000,0	400,0	2	120	264	35	38178	41,1	380,16	6,07	2309,3
-105,0	35786	57,6	68,0	43,7	39000,0	800,0	2	480	124	35	38178	41,1	714,24	6,07	4338,7
-105,0	35786	57,6	68,0	43,7	39000,0	1600,0	2	480	248	35	38178	41,1	1428,48	6,07	8677,4
-105,0	35786	57,6	68,0	43,7	39000,0	2000,0	2	960	148	35	38178	41,1	1704,96	6,07	10356,9

Figure 18 Downlink (GEO to ground station) link budget for 6G timeframe

4.4.2.3 5G timeframe - Ground station to LEO

For the same reasoning as for the feeder links in Ka-band, the bandwidth for the LEO satellites is set to 400 MHz. The resulting SNR is high, so the bandwidth can be further increased.

Uplink - FR2: LEO 600 km, elevation angle 30°																	
UE		Satellite										Results - 5G NR Performance					
max. EIRP [dBW]	max. EIRP Density [dBW/MHz]	Antenna Gain [dBi]	G/T [dB/K]	Altitude [km]	Frequency [MHz]	max. available BW [MHz]	FR	SCS [kHz]	N_{RB}	Elevation angle [°]	Slant range [km]	CNR [dB]	max. eff. BW [MHz]	eff. BW [MHz]	Count of RB with a BW of 11,52 MHz	Spectral Efficiency [Bit/s/Hz]	max. Datarate [Mbit/s]
80,00	54,2	34,9	9,1	600	29000,0	400	2	960	33	30	1075	41,8	380,16	380,16	33	6,67	2534,60

Figure 19 5G timeframe uplink (ground station to LEO) link budget

With a bandwidth of 400 MHz in the downlink, the same data rate can be achieved as in the uplink.

Downlink - FR2: LEO 600 km, elevation angle 30°															
Satellite			UE									Results			
PFD [dBW/m²]	Altitude [km]	max. EIRP Density [dBW/MHz]	Antenna Gain [dBi]	G/T [dB/K]	Frequency [MHz]	max. BW [MHz]	FR	SCS [kHz]	N_{RB}	Elevation angle [°]	Slant rage [km]	CNR [dB]	max. eff. BW [MHz]	Spectral Efficiency - 5G NTN [Bit/s/Hz]	max. Datarate - 5G NTN [Mbit/s]
-105,0	600	26,6	64,3	40,0	19000,0	100,0	2	120	66	30	1075	48,3	95,04	6,07	577,3
-105,0	600	26,6	64,3	40,0	19000,0	200,0	2	120	132	30	1075	48,3	190,08	6,07	1154,7
-105,0	600	26,6	64,3	40,0	19000,0	400,0	2	120	264	30	1075	48,3	380,16	6,07	2309,3
-105,0	600	26,6	64,3	40,0	19000,0	800,0	2	480	124	30	1075	48,3	714,24	6,07	4338,7
-105,0	600	26,6	64,3	40,0	19000,0	1600,0	2	480	248	30	1075	48,3	1428,48	6,07	8677,4
-105,0	600	26,6	64,3	40,0	19000,0	2000,0	2	960	148	30	1075	48,3	1704,96	6,07	10356,9

Figure 20 5G timeframe downlink (LEO to ground station) link budget

4.4.2.4 6G timeframe - Ground station to LEO

Since the bandwidth of 2 GHz is available in the Q/V band, the link budgets are calculated with 2 GHz bandwidth. In this case, too, the maximum spectral efficiency can be achieved. This results in a data rate of 11.367 Gbit/s per feeder link can be achieved.

Uplink - FR2: LEO 600 km, elevation angle 30°																	
UE		Satellite										Results - 5G NR Performance					
max. EIRP [dBW]	max. EIRP Density [dBW/MHz]	Antenna Gain [dBi]	G/T [dB/K]	Altitude [km]	Frequency [MHz]	max. available BW [MHz]	FR	SCS [kHz]	N_{RB}	Elevation angle [°]	Slant range [km]	CNR [dB]	max. eff. BW [MHz]	eff. BW [MHz]	Count of RB with a BW of 11,52 MHz	Spectral Efficiency [Bit/s/Hz]	max. Datarate [Mbit/s]
81,00	48,7	39,1	13,3	600	47000,0	2000	2	960	148	30	1075	31,3	1704,96	1704,96	148	6,67	11367,31

Figure 21 6G timeframe uplink (ground station to LEO) link budget

The maximum spectral efficiency is not achieved in the downlink. Since the transmission power on the satellite side is determined by the defined PFD limits, the link budget can be improved with a better G/T on the gateway side.

Downlink - FR2: LEO 600 km, elevation angle 30°															
Satellite			UE									Results			
PFD [dBW/m²]	Altitude [km]	max. EIRP Density [dBW/MHz]	Antenna Gain [dBi]	G/T [dB/K]	Frequency [MHz]	max. BW [MHz]	FR	SCS [kHz]	N_{RB}	Elevation angle [°]	Slant rage [km]	CNR [dB]	max. eff. BW [MHz]	Spectral Efficiency - 5G NTN [Bit/s/Hz]	max. Datarate - 5G NTN [Mbit/s]
-105,0	600	26,6	59,4	35,1	39000,0	100,0	2	120	66	30	1075	31,7	95,04	5,39	511,9
-105,0	600	26,6	59,4	35,1	39000,0	200,0	2	120	132	30	1075	31,7	190,08	5,39	1023,7
-105,0	600	26,6	59,4	35,1	39000,0	400,0	2	120	264	30	1075	31,7	380,16	5,39	2047,5
-105,0	600	26,6	59,4	35,1	39000,0	800,0	2	480	124	30	1075	31,7	714,24	5,39	3846,7
-105,0	600	26,6	59,4	35,1	39000,0	1600,0	2	480	248	30	1075	31,7	1428,48	5,39	7693,5
-105,0	600	26,6	59,4	35,1	39000,0	2000,0	2	960	148	30	1075	31,7	1704,96	5,39	9182,5

Figure 22 6G timeframe downlink (LEO to ground station) link budget

4.4.3 Comparison with target values

In Table 21, the expected data rates as defined in chapter 3.1 are compared with the results from the link budget calculation. For the GEO satellite feeder links, all expectations can be met, even if the expected values for the 5G timeframe were assumed for a bandwidth of 500 MHz and the calculated values with a bandwidth of 400 MHz. This is due to a very good link budget and thus a high SNR, so that the maximum spectral efficiency can be achieved in both the uplink and the downlink.

A comparison with a modern satellite, for example the digital transparent KONNECT VHTS (Very High Throughput Satellite) of EUTELSAT, which deliver a total capacity of 500 Gbit/s, shows that 100 feeder links (each 400 MHz and dual polarized) are necessary to ensure this data rate. The implementation of the feeder links in the Ka-band for such a satellite would be very cost-intensive, so that the feeder links of the KONNECT VHTS are realized in the Ka and Q/V band using DVB-S2X as air interface. According to our link budget calculations with the 5G NR air interface, 23 gateways would be needed to reach the total capacity of 500 Gbit/s.

		5G timeframe		6G timeframe	
		Expected	Achievable	Expected	Achievable
GEO	UL data rate [Gbit/s]	2,00	2,53	8,00	11,37
	DL data rate [Gbit/s]	0,50	2,31	2,00	10,36
LEO	UL data rate [Gbit/s]	7,42	2,53	37,10	11,37
	DL data rate [Gbit/s]	0,21	2,31	1,06	9,18

Table 21 Expected vs. achievable data rates for 5G and 6G timeframe

In comparison to the GEO feeder links, where the expected data rates were calculated per 500 MHz bandwidth, the data rate for the LEO feeder links was calculated based on the required data rate of the user links. Therefore, the expected data rate is to be understood as the total data rate. In the 5G timeframe, two feeder links (each with 400 MHz bandwidth and two polarizations) would be needed to achieve the required capacity. The same applies to the 6G timeframe, where the 2 GHz bandwidth in the Q/V band is used.

5 Technology components

This section provides description of aspects relevant to multiple links within the 3D architecture. Section 5.1 describes multi technology connectivity for aerial vehicles, and section 5.2 describes free-space optics.

5.1 Multi technology connectivity

Aerial vehicles (AVs) such as electric vertical take-off and landing (eVTOL) aircraft will make aerial passenger transportation a reality in urban environments. However, their communication connectivity is still under research to realize their safe and full-scale operation. This paper envisages a multi-connectivity (MC) enabled aerial network to provide ubiquitous and reliable service to AVs. Vertical heterogeneous networks with direct air-to-ground (DA2G) and air-to-air (A2A) communication, high altitude platforms (HAPs), and low Earth orbit (LEO) satellites are considered.

We evaluate the end-to-end (E2E) multi-hop reliability and network availability of the downlink of AVs for remote piloting scenarios, and control/telemetry traffic. Command and control (C2) connectivity service requires ultra-reliable and low-latency communication (URLLC), therefore we analyse E2E reliability and latency under the finite blocklength (FBL) regime. We explore how different MC options satisfy the demanding E2E connectivity requirements taking into account antenna radiation patterns and unreliable backhaul links. Since providing seamless connectivity to AVs is very challenging due to the line-of-sight (LoS) interference and reduced gains of downtilt ground base station (BS) antennas, we use coordinated multi-point (CoMP) among ground BSs to alleviate the intercell interference.

Beyond visual line of sight (BVLOS) remote piloting of an AV requires a communication path between the remote pilot and the AV. In this concept, ground pilots remotely navigate an AV, which can supply pilots with a first-person view by onboard cameras and other useful sensor data. Remote piloting operation emphasizes the demand for resilient E2E communication paths from the remote pilots to the AVs. As eVTOLs and UAVs occupy the sky, they must coordinate with one another as well as other AVs to efficiently share the low-altitude sky. Unmanned traffic management (UTM) introduces the regulation of these vehicles in a more-autonomous manner compared with air traffic management (ATM). Machine-type communications (MTC) can become the dominant connectivity type in UTM rather than human-centric ATM communication in the future [24]. Based on [24], control/telemetry traffic for remote piloting operations of eVTOLs requires a data rate of about 0.25~1 Mbps, E2E latency of less than 10ms~1sec , and a minimum communication reliability of 99.999%.

5.1.1 Key Performance Indicators

The most important KPIs related to URLLC are latency, reliability, and network availability. Latency is defined as the delay a packet experiences from the ingress of a protocol layer at the transmitter to the egress of the same layer at the receiver [25]. In the URLLC literature, the reliability is reflected either by packet loss probability or by latency, which we call them error-based and delay-based reliability, respectively. The E2E packet loss probability, $\mathcal{E}_{\mathrm{E2E}}$, includes different components such as backhaul failure probability, queueing delay violation, decoding error probability, and so on. Therefore, in error-based reliability, the reliability requirement which is defined by

$$\mathcal{R} = 1 - \mathcal{E}_{\mathrm{E2E}}$$

can be satisfied if the overall packet loss probability does not exceed $\varepsilon^{\mathrm{th}}$. On the other hand, using the convention that dropped packets have infinite latency, authors of [25] define the reliability as the probability that the latency does not exceed a pre-defined threshold D^{th}. Thus, in delay-based reliability

$$\mathcal{R} = \Pr\left\{\mathcal{D}_{\mathrm{E2E}} \le D^{\mathrm{th}}\right\}$$

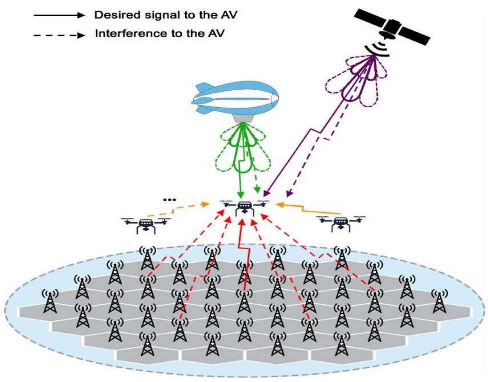

Figure 23 System model.

where $\mathcal{D}_{\mathrm{E2E}}$ is the E2E delay from the transmitter to the receiver.

Different from latency and reliability, which are the QoS required by each user, availability captures the performance of the network how it can respond to the demands of the users, and is another key performance metric for URLLC. In the conventional systems, availability is specified by the packet loss probability which we call it error-based network availability, i.e.,

$$P_{\mathrm{A}} = \Pr\left\{\mathcal{E}_{\mathrm{E2E}} \le \varepsilon^{\mathrm{th}}\right\}$$

However, for URLLC services, availability is defined as the probability that the network can support a service with a target QoS requirement on both latency and reliability [26]. Based on the above definitions, the availability for URLLC services can be described by the following equation, which we call it as delay-aware network availability

$$P_{\mathrm{A}} = \Pr\left\{\mathcal{E}_{\mathrm{E2E}} \le \varepsilon^{\mathrm{th}}, \mathcal{D}_{\mathrm{E2E}} \le D^{\mathrm{th}}\right\}$$

Here $\varepsilon^{\mathrm{th}}$ and D^{th} characterize the QoS requirements in terms of packet error and delay.

5.1.2 Multi-connectivity

MC using multiple communication paths simultaneously is the key technology to reduce latency and increase reliability to fulfill strict requirements of AVs' remote piloting. As shown in Figure 23, the system model consists of an integration of multiple RATs including DA2G, A2A, HAP, and LEO satellite communication. For all the RATs, we assume particular frequency band with full frequency reuse such that each link experiences probabilistic interference from all the corresponding links. The E2E path of each RAT is illustrated in Figure 24, a directive path starting with the core network, traversing the backhaul link and the radio link (downlink) to reach the destination AV, which is the AV that remote pilot wants to navigate. The communication links consist of ground BS-to-AV (G2A), HAP ground station-to-HAP (G2H), satellite ground station-to-LEO satellite (G2S), and AV/HAP/LEO satellite-to-AV (A2A/H2A/S2A). In Figure 24, four different E2E paths are shown, i.e., the red line which illustrates "DA2G E2E path" includes the backhaul link to the ground BS and G2A link. "A2A E2E path", illustrated with orange line is defined as the path consisting of backhaul, G2A and A2A links. The green line illustrates the "HAP E2E path" defined as the path consisting of backhaul link to the HAP ground station, G2H and H2A links. Finally, the "LEO satellite E2E path" indicated with violet line includes the backhaul link to the satellite ground station, G2S and S2A links.

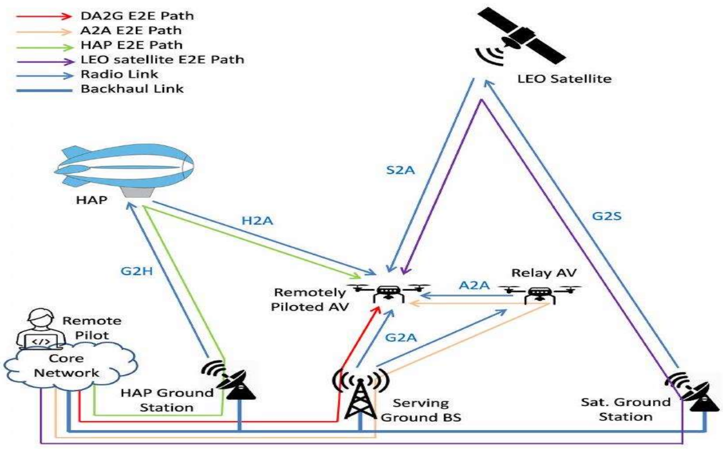

Figure 24 Illustration of mult-RAT and E2E communication paths.

5.1.3 Transmission and Combining Strategy

We consider packet cloning for transmitting the message from the remote pilot to the AV over independent links. In this approach, the source sends copies of the message through each of the available links [27]. The combining scheme is joint decoding, where each link is decoded individually. Thus, the overall packet loss probability of N parallel transmission paths is

$$\mathcal{E}_{\mathrm{E2E}} = \prod_{i=1}^{N} \mathcal{E}_{\mathrm{E2E}}^{i}$$

where $\mathcal{E}_{\mathrm{E2E}}^{i}$ is the error probability of the i th path, and $i \in \{\mathrm{g}, \mathrm{a}, \mathrm{h}, \mathrm{s}\}$ refers to different RATs including DA2G, A2A, HAP, and satellite communications, respectively. It also potentially reduces the delay, since only the packet that arrives earlier and is decoded correctly needs to be considered. Hence, the E2E delay of multi-RAT using the cloning scheme is calculated as [27]

$$\mathcal{D}_{\mathrm{E2E}} = \min_{i=1,\ldots,N} \{\mathcal{D}_{\mathrm{E2E}}^{i}\}$$

where $\mathcal{D}_{\mathrm{E2E}}^{i}$ is the E2E delay of the i th path.

5.1.4 SINR calculation

One may obtain the channel coefficient between any two nodes x and y as

$$h_{\mathrm{xy}} = \left(\frac{g_{\mathrm{xy}}}{PL_{\mathrm{xy}}}\right)^{1/2} \omega_{\mathrm{xy}}$$

where g_{xy} is the total antenna gain between nodes x and y given by the product of their respective antenna gains. Finally, the SINR of X2Y link with bandwidth B^{xy}, xy $\in \{\mathrm{ga}, \mathrm{aa}\}$, is calculated as follows

$$\gamma^{\mathrm{xy}} = \frac{p_{\mathrm{x}} |h_{\mathrm{xy}}|^2}{P_{\mathrm{interf}} \sum_{i \in \mathcal{N}_i} p_{\mathrm{x}_i} |h_{\mathrm{x}_i \mathrm{y}}|^2 + B^{\mathrm{xy}} N_0}$$

where p_{x} is the transmit power of node x, and N_0 is the noise spectral density. $\mathcal{N}_i$ is the set of interfering nodes and, $h_{\mathrm{x}_i\mathrm{y}}$ indicates the channel coefficient between the interfering node x_i and node y. We assume that interference cancellation techniques can harness interference [30], [31], [32], and it can be explicitly captured by interference probability denoted by P_{interf}. It points out that the higher the interference cancellation, the lower the interference probability. Hence, the effect of interference power on the network is affected by P_{interf} due to the fact that each potential interferer is modeled as a Bernoulli random variable with a probability of P_{interf}. We also assume that the G2H and the G2S links are interference-free, while the interference on H2 A/S2 A links is due to the side lobes of HAP/satellite's antenna overlapping with the main lobes [28], [29].

For the channel models utilized in this section, please refer to our paper in [33].

5.1.5 Reliability and Latency Analysis

5.1.5.1 Transmission Analysis in the FBL Regime

The achievable data rate of the X2Y link, R^{xy}, with FBL coding and an acceptable Block Error Rate (BLER) $\varepsilon_{\mathrm{t}}^{\mathrm{xy}}$, xy ∈ {ga, aa, gh, ha, gs, sa}, has an approximation as [34]

$$\mathrm{R}^{xy} \approx \mathrm{B}^{xy}\left(C^{xy} - \sqrt{\frac{V^{xy}}{B^{xy} D_t^{xy}}} \frac{Q^{-1}(\epsilon_t^{xy})}{ln2}\right) bits/s$$

where $C^{\mathrm{xy}} = \log_2(1+\gamma^{\mathrm{xy}})$ is the Shannon capacity and $V^{\mathrm{xy}} = 1-(1+\gamma^{\mathrm{xy}})^{-2}$ is the channel dispersion. Moreover, $D_{\mathrm{t}}^{\mathrm{xy}}$ is the transmission delay of the X2Y link, and $Q^{-1}(\cdot)$ refers to the inverse Gaussian Q-function $Q(x) = \frac{1}{\sqrt{2\pi}}\int_x^{\infty} e^{-\frac{t^2}{2}}\,\mathrm{d}t$.

In the FBL regime, decoding error probability is given by

$$\varepsilon_{\mathrm{t}}^{\mathrm{xy}} \approx Q\left(f\left(\gamma^{\mathrm{xy}}, R^{\mathrm{xy}}, D_{\mathrm{t}}^{\mathrm{xy}}\right)\right)$$

where

$$f\left(\gamma^{\mathrm{xy}}, R^{\mathrm{xy}}, D_{\mathrm{t}}^{\mathrm{xy}}\right) \triangleq \frac{(B^{\mathrm{xy}}C^{\mathrm{xy}} - R^{\mathrm{xy}})\ln 2}{\sqrt{B^{\mathrm{xy}}V^{\mathrm{xy}}/D_{\mathrm{t}}^{\mathrm{xy}}}}$$

When transmitting a packet that contains b bits over the allocated channel, the decoding error probability can be obtained by substituting $D_{\mathrm{t}}^{\mathrm{xy}} = \frac{b}{R^{\mathrm{xy}}}$ into $\varepsilon_{\mathrm{t}}^{\mathrm{xy}}$ expression. The above expressions are for AWGN channels which contain no fading. Here, we can assume our channel as a quasi-static flat fading channel such that at each realization, its characteristics remain the same.

By adopting ARQ scheme, the packet is retransmitted until it is received correctly, and we assume that there is reliable feedback from the AV to the transmitter as in [35]. Hence, the average transmission delay of the X2Y link is calculated as

$$\bar{D}_{\mathrm{t}}^{\mathrm{xy}} = \frac{D_{\mathrm{t}}^{\mathrm{xy}}}{1-\varepsilon_{\mathrm{t}}^{\mathrm{xy}}}$$

5.1.5.2 Queueing Analysis

As stated in [34], the packet arrival process to the BS in MTC, which is an aggregation of packets generated by multiple sensors, can be modeled as a Poisson process. The event that each sensor at any given instant has a packet to upload or not is modeled as a Bernoulli process. The probability that sensor m has a packet to upload is denoted by P_m. Then, the arrival process to the BS is defined as a Poisson process, because the sensors are independent. Since MTC is the connectivity type in our scenario, each remote pilot resembles a sensor that at any time instant may deliver a packet to the AV of interest via node x. Therefore, if assume that $M_{\mathrm{X}}\mathrm{AV}$ s are served by node x, where $\mathrm{x} \in \{\mathrm{g}, \mathrm{a}, \mathrm{h}, \mathrm{s}\}$ refers to ground BS, relay AV, HAP, and LEO satellite, respectively, the average total arrival rate to node x is $\lambda_{\mathrm{x}} = \sum_{m=1}^{M_{\mathrm{x}}} P_m$ packets/s.

Denote the packet dropping probability due to queueing delay violation as

$$\varepsilon_{\mathrm{q}}^{\mathrm{x}} = \Pr\left\{D_{\mathrm{q}}^{\mathrm{x}} > D_{\mathrm{q,max}}\right\}$$

where $D_{\mathrm{q}}^{\mathrm{x}}$ is the queue delay of node x, and $\mathrm{x} \in \{\mathrm{g}, \mathrm{a}, \mathrm{h}, \mathrm{s}\}$. As described above, the packet arrival process to node x can be modeled as a Poisson process with the average arrival rate of λ_{x} packets/s.

Then, the effective bandwidth of node x, which is the minimal constant packet service rate required to satisfy the queueing delay requirement $\left(D_{\mathrm{q,max}}, \varepsilon_{\mathrm{q}}^{\mathrm{x}}\right)$ can be expressed as follows [34]

$$E_{\mathrm{BW}}^{\mathrm{x}} = \frac{\ln\left(1/\varepsilon_{\mathrm{q}}^{\mathrm{x}}\right)}{D_{\mathrm{q}}^{\mathrm{x}} \ln\left[\frac{\ln\left(1/\varepsilon_{\mathrm{q}}^{\mathrm{x}}\right)}{\lambda_{\mathrm{x}} D_{\mathrm{q}}^{\mathrm{x}}} + 1\right]} \text{ packets /s}$$

5.1.6 E2E Delay and Packet Loss Probability

5.1.6.1 E2E Path Through DA2G Communication

The E2E delay of DA2G path consists of delay due to backhaul link, D_{b}, queue delay in the ground BS, $D_{\mathrm{q}}^{\mathrm{g}}$, and the average transmission delay of the G2A link, $\bar{D}_{\mathrm{t}}^{\mathrm{ga}}$. Hence, the E2E delay requirement can be satisfied with the following constraint

$$D_{\mathrm{b}} + D_{\mathrm{q}}^{\mathrm{g}} + \bar{D}_{\mathrm{t}}^{\mathrm{ga}} \leq D^{\mathrm{th}}$$

By deploying fiber optic backhaul links, we assume that the backhaul delay for remote piloting is around $1\ \mathrm{ms}$[1].

Correspondingly, the overall packet loss probability is due to the backhaul failure, packet dropping in the ground BS's queue with a probability of $\varepsilon_{\mathrm{q}}^{\mathrm{g}}$, and decoding error of the G2A link with a probability of $\varepsilon_{\mathrm{t}}^{\mathrm{ga}}$. Thus, reliability can be guaranteed if

$$1 - (1 - \varepsilon_{\mathrm{b}})\left(1 - \varepsilon_{\mathrm{q}}^{\mathrm{g}}\right)\left(1 - \varepsilon_{\mathrm{t}}^{\mathrm{ga}}\right) \leq \varepsilon^{\mathrm{th}}$$

ε_{b} is the failure probability of backhaul link, which is modeled by a Bernoulli process, and $1 - \varepsilon^{\mathrm{th}}$ is the required reliability.

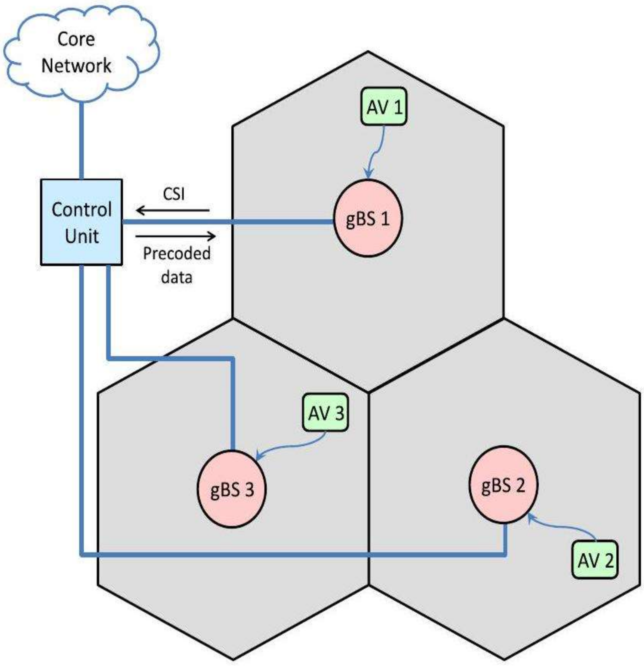

Figure 25 Illustration of centralized CoMP architecture with cluster size of N=3.

5.1.6.2 E2E Communication Path of JT CoMP

Here, we consider a CoMP cluster, consisting of N ground BSs that are serving M AVs, where $M \leq N$. The E2E delay requirement of JT CoMP with a centralized architecture, introduced in [36], is given by

$$D_{\mathrm{b}} + D_{\mathrm{c}} + D_{\mathrm{q}}^{\mathrm{g}} + \bar{D}_{\mathrm{t}}^{\mathrm{JT}} \leq D^{\mathrm{th}}$$

where D_{b} as before is the backhaul delay from the core network to the serving ground BSs, and

$$D_{\mathrm{c}} = \max_{n}\{D_{\mathrm{f}}^{\mathrm{g}n} + D_{\mathrm{b}}^{\mathrm{C}} + D_{\mathrm{b}}^{\mathrm{D}}\}$$

is the delay due to CoMP, cf. Figure 25 , consisting of the delay that $\mathrm{AV}m, m \in \{1, \dots, M\}$, feeds back its channel state information (CSI) to its serving $\mathrm{BS}n, n \in \{1, \dots, N\}$, i.e., $D_{\mathrm{f}}^{\mathrm{g}n}$, and the backhaul delay between ground BS n and the control unit (CU) when ground BS n forwards the local CSI to the CU, i.e., $D_{\mathrm{b}}^{\mathrm{C}}$, and the backhaul delay between CU and ground BS n when the CU distributes precoded data to ground BS n, i.e., $D_{\mathrm{b}}^{\mathrm{D}}$. The feedback delay as in [37] is considered a fixed value of $5\ \mathrm{ms}$, and we assume the backhaul delay between the ground BS and CU as $D_{\mathrm{b}}^{\mathrm{C}} = D_{\mathrm{b}}^{\mathrm{D}} = 0.1\mathrm{ms}.$ [2] Moreover, $\bar{D}_{\mathrm{t}}^{\mathrm{JT}} = \frac{D_{\mathrm{t}}^{\mathrm{ga}}}{1-\varepsilon_{\mathrm{t}}^{\mathrm{JT}}}$ is the transmission delay of JT CoMP

The overall packet loss probability of JT with a CoMP cluster size of N can be calculated as

$$1 - (1 - \varepsilon_{\mathrm{b}})\left(1 - \prod_{n=1}^{N} \varepsilon_{\mathrm{c}}^{\mathrm{g}n}\right)\left(1 - \prod_{n=1}^{N} \varepsilon_{\mathrm{q}}^{\mathrm{g}n}\right)\left(1 - \varepsilon_{\mathrm{t}}^{\mathrm{JT}}\right) \leq \varepsilon^{\mathrm{th}}$$

where $\varepsilon_{\mathrm{C}}^{\mathrm{g}n}$ is the probability that ground $\mathrm{BS}n$ fails to cooperate in its CoMP cluster and is given by [36]

$$\varepsilon_{\mathrm{c}}^{gn} = \varepsilon_{\mathrm{b}}^{\mathrm{D}} + \left(1 - \varepsilon_{\mathrm{b}}^{\mathrm{D}}\right) \prod_{n=1}^{N} \left(\varepsilon_{\mathrm{b}}^{\mathrm{C}} + \left(1 - \varepsilon_{\mathrm{b}}^{\mathrm{C}}\right) \varepsilon_{\mathrm{f}}^{gn}\right)$$

$\varepsilon_{\mathrm{b}}^{\mathrm{D}}$ is the failure probability of the backhaul link between the CU and ground BS n when the CU transmits precoded data to ground $\mathrm{BS}n$, and $\varepsilon_{\mathrm{b}}^{\mathrm{C}}$ is the failure probability of the backhaul link between ground BS n and the CU when ground $\mathrm{BS}n$ forwards the local CSI to the CU. $\varepsilon_{\mathrm{f}}^{gn}$ is the link failure probability of the access link between AV m and ground BS n, when the AV feeds back the CSI to ground BS n. We suppose that the CSI feedback is error free, i.e., $\varepsilon_{\mathrm{f}}^{gn} \approx 0$, so the channel coefficients between all the AVs and their serving ground BSs are perfectly known at the CU.

Finally, $\varepsilon_{\mathrm{t}}^{\mathrm{JT}}$ denotes the decoding error probability of JT CoMP and is calculated by $\varepsilon_{\mathrm{t}}^{\mathrm{JT}} \approx Q\left(f\left(\gamma^{\mathrm{JT}}, R^{\mathrm{ga}}, D_{\mathrm{t}}^{\mathrm{ga}}\right)\right)$, where γ^{JT} is the SINR of $\mathrm{AV}m$ given by

$$\gamma^{\mathrm{JT}} = \frac{p_m}{P_{\text{interf}} \sum_{i \in \mathcal{N}_i} p_i |h_i|^2 + B^{\mathrm{ga}} N_0}$$

p_m denotes the symbol power allocated to $\mathrm{AV}m$ and based on equal power strategy is derived as [38]

$$p_m = \frac{P_{\max}}{\max[\mathrm{WW}^*]_{j,j}}$$

W is the zero-forcing precoding obtained as the pseudo-inverse of the channel matrix, $\mathrm{H} \in \mathbb{C}^{M \times N}$, available at the CU, i.e., $\mathrm{W} = \mathrm{H}^*(\mathrm{HH}^*)^{-1}$ where (.)* denotes the conjugate transpose. We assume disjoint CoMP clusters with intercluster interference, where p_i in (33) is the transmit power of interfering BS i, with ground BS's power constraint $P_{\max}$. As the worst case of the SINR we assume $p_i = P_{\max}$. Since we assume perfect CSI at the CU, the intra-cluster interference due to serving other AV s in the same CoMP cluster is canceled by the zero-forcing precoding.

5.1.6.3 E2E Path Through A2A Communication

For the scenario of deploying an AV as a relay to transmit data to the AV of interest, the packet in addition to the DA2G communication path goes across relay AV's queue, with a delay of $D_{\mathrm{q}}^{\mathrm{a}}$, and A2A link, with an average delay of $\bar{D}_{\mathrm{t}}^{\mathrm{aa}}$. Hence, the delay components should satisfy

$$D_{\mathrm{b}} + D_{\mathrm{q}}^{\mathrm{g}} + \bar{D}_{\mathrm{t}}^{\mathrm{ga}} + D_{\mathrm{q}}^{\mathrm{a}} + \bar{D}_{\mathrm{t}}^{\mathrm{aa}} \le D^{\mathrm{th}}$$

Correspondingly, the reliability of the A2A communication path can be ensured if

$$1 - (1 - \varepsilon_{\mathrm{b}})\left(1 - \varepsilon_{\mathrm{q}}^{\mathrm{g}}\right)\left(1 - \varepsilon_{\mathrm{t}}^{\mathrm{ga}}\right)\left(1 - \varepsilon_{\mathrm{q}}^{\mathrm{a}}\right)\left(1 - \varepsilon_{\mathrm{t}}^{\mathrm{aa}}\right) \le \varepsilon^{\mathrm{th}}.$$

If we consider a swarm of parallel coordinated AVs with single-hop transmission to serve the desired AV with joint decoding strategy, the E2E error probability and delay can be calculated by (5) and (6), respectively. In fact, it helps increase reliability by exploiting path diversity in the A2A link. 4) E2E Path Through HAP Communication: For HAP, long distances of G2H and H2A links cause propagation delay in addition to previous delay components. Therefore, the E2E delay requirement of HAP is satisfied if

$$D_{\mathrm{b}} + D_{\mathrm{q}}^{\mathrm{g}} + \bar{D}_{\mathrm{t}}^{\mathrm{gh}} + D_{\mathrm{p}}^{\mathrm{gh}} + D_{\mathrm{q}}^{\mathrm{h}} + \bar{D}_{\mathrm{t}}^{\mathrm{ha}} + D_{\mathrm{p}}^{\mathrm{ha}} \leq D^{\mathrm{th}}$$

where $D_{\mathrm{p}}^{\mathrm{gh}}$ and $D_{\mathrm{p}}^{\mathrm{ha}}$ are the propagation delay of the G2H link and the H2A link, respectively. $\bar{D}_{\mathrm{t}}^{\mathrm{ha}}$ denotes the average transmission delay of the H2A link.

The overall packet loss probability of the HAP communication, similar to the A2A communication, can be computed as

$$1 - (1 - \varepsilon_{\mathrm{b}})(1 - \varepsilon_{\mathrm{q}}^{\mathrm{g}})\left(1 - \varepsilon_{\mathrm{t}}^{\mathrm{gh}}\right)(1 - \varepsilon_{\mathrm{q}}^{\mathrm{h}})(1 - \varepsilon_{\mathrm{t}}^{\mathrm{ha}}) \leq \varepsilon^{\mathrm{th}}$$

5.1.6.4 E2E Path Through LEO Satellite Communication

The E2E delay constraint of LEO satellite path, similar to the HAP communication, is given by

$$D_{\mathrm{b}} + D_{\mathrm{q}}^{\mathrm{g}} + \bar{D}_{\mathrm{t}}^{\mathrm{gs}} + D_{\mathrm{p}}^{\mathrm{gs}} + D_{\mathrm{q}}^{\mathrm{s}} + \bar{D}_{\mathrm{t}}^{\mathrm{sa}} + D_{\mathrm{p}}^{\mathrm{sa}} \leq D^{\mathrm{th}}$$

where $D_{\mathrm{p}}^{\mathrm{gs}}$ and $D_{\mathrm{p}}^{\mathrm{sa}}$ are the propagation delay of the G2 S and S2A links, respectively. $\bar{D}_{\mathrm{t}}^{\mathrm{sa}}$ denotes the average transmission delay of the S2A link.

Due to movement of LEO satellite, in addition to the aforementioned factors, the reliability depends on the availability of LEO satellite links and can be guaranteed if

$$1 - (1 - \varepsilon_{\mathrm{b}})(1 - \varepsilon_{\mathrm{q}}^{\mathrm{g}})(1 - \varepsilon_{1}^{\mathrm{gs}})(1 - \varepsilon_{\mathrm{t}}^{\mathrm{gs}})(1 - \varepsilon_{\mathrm{q}}^{\mathrm{s}})(1 - \varepsilon_{\mathrm{l}}^{\mathrm{sa}})(1 - \varepsilon_{\mathrm{t}}^{\mathrm{sa}}) \leq \varepsilon_{\mathrm{th}}$$

$\varepsilon_{1}^{\mathrm{xy}}, \mathrm{xy} \in \{\mathrm{gs}, \mathrm{sa}\}$ is the unavailability probability of LEO satellite X2Y link, which is defined as $1 - P_{\mathrm{vis}}^{\mathrm{xy}}$. Here, we approximate the link availability probability with visibility probability which is given by [39]

$$P_{\mathrm{vis}}^{\mathrm{xy}} = 1 - \left(1 - \frac{d_{\mathrm{max}}^{\mathrm{xy}} - \hbar_{\mathrm{s}}^{2}}{4R_{\mathrm{e}}(R_{\mathrm{e}} + \hbar_{\mathrm{s}})}\right)^{n_{\mathrm{s}}}$$

where $d_{\mathrm{max}}^{\mathrm{xy}}$ is the maximum distance between nodes x and y at the minimum elevation angle ϑ_{min}. Moreover, R_{e} is the Earth radius, $\hbar_{\mathrm{s}}$ and n_{s} are altitude and the number of LEO satellites, respectively.

5.1.7 Simulation Assumptions

In this section, we evaluate the performance of different E2E connectivity paths comprising multiple RATs and investigate how MC can ensure the stringent requirements of remote piloting the eVTOLs. To this end, we consider an urban scenario with macro cells for the ground network. The system parameters are listed in Table 22.

Table 22 System Parameters.

System parameter	Value
Required reliability, $1 - \varepsilon^{\mathrm{th}}$	0.99999
Delay threshold, D^{th}	20 ms

Packet size, b	32 bytes
Average packet arrival rate of AV, λ_a	100 packets/s [34]
Average packet arrival rate of gBS, λ_g	1000 packets/s [34]
Average packet arrival rate of HAP, λ_h	10000 packets/s [40]
Average packet arrival rate of satellite, λ_s	10000 packets/s
Queueing delay bound, D^{q}_{max}	0.7 ms
Queueing delay violation probability, ε^{x}_{q}	10^{-6}
Backhaul failure probability, ε_b	10^{-6}[40]
Carrier frequency of all links in S-band, f_c	2 GHz
Carrier frequency of satellite links in Ka-band, f_c	30 GHz
AV Tx power	23 dBm[41]
gBS/HAP Tx power	46 dBm[41]
LEO Tx power	50 dBm[42]
AV Tx/Rx antenna gain, g_a	0 dBi[41]
Maximum gain of gBS antenna element, g^{max}_{e}	8 dBi[43]
Maximum gain of HAP Tx/Rx antenna, g^{max}_{h}	32 dBi[40]
Maximum gain of LEO Tx/Rx antenna, g^{max}_{s}	38 dBi
AV Rx noise figure	9 dB[41]
HAP/LEO Rx noise figure	5 dB[41]
Number of gBS antenna elements, N_e	8 [43]
Downtilt angle, ϕ_t	102°[43]
Inter-site distance (ISD)	500 m[41]
Height of gBS, $\hbar_g$	25 m[41]
Altitude of AV, $\hbar_a$	300 m[24]
Altitude of HAP, $\hbar_h$	20 km[24]
Altitude of LEO satellite, $\hbar_s$	1110 km[46]
Number of LEO satellites, n_s	4425[46]
Minimum elevation angle, ϑ_{min}	15°[47]

Rice factor of G2A link, K_{ga}	$5 \sim 12$ dB[40]
Rice factor of A2A link, K_{aa}	12 dB[40]
Rice factor of G2H link, K_{gh}	$5 \sim 15$ dB[40]
Rice factor of H2A link, K_{ha}	$12 \sim 15$ dB[40]
Rice factor of G2S link, K_{gs}	$5 \sim 15$ dB (S-band), $10 \sim 30$ dB (Ka-band)
Rice factor of S2A link, K_{sa}	$12 \sim 15$ dB (S-band), $20 \sim 30$ dB (Ka-band)
Noise spectral density, N_0	-174 dBm/Hz
LoS (NLoS) shadow fading standard deviation	4 (6)dB [41]

The resource blocks (RBs) assigned to each AV consist of 4 consecutive RBs. The subcarrier spacing is 0.2 MHz. Therefore, the allocated bandwidth of the X2Y link, B^{xy}, xy $\in \{ga, aa, ha, sa\}$, to transmit a packet is 0.8 MHz, which does not exceed the coherence bandwidth of 1.2 MHz [44]. The dedicated bandwidth of the G2H/G2S link, B^{gh}/B^{gs}, is assumed to be fixed as 1 MHz. The queueing delay requirement is considered as $D_{q,max} = 0.7$ ms and $\varepsilon_q^x = 10^{-6}$ for x $\in \{a, g, h, s\}$. The average packet arrival rate of AV, ground BS, HAP, and satellite is assumed as $\lambda_a = 100$ packets/s, $\lambda_g = 1000$ packets /s, and $\lambda_h = \lambda_s = 10000$ packets/s, respectively. So based on (26), the effective bandwidth of the arrival process to satisfy the queueing delay requirement is determined as $E_{BW}^a \approx 3700$ packets/s, $E_{BW}^g \approx 6500$ packets/s, and $E_{BW}^h = E_{BW}^S \approx 18000$ packets /s. We consider the data rate of all the links, R^{xy}, as 500 kbps. In addition, probability of interference, P_{interf} , and CoMP cluster size, N, are assumed 0.05 and 3, respectively. In our simulations, the system parameters in most cases are as specified above or listed in Table I, unless otherwise stated.

We consider a hexagonal grid for the cellular terrestrial network consisting of 3 tiers, i.e., 37 cells in total. 10 AVs are located randomly with uniform distribution at a fixed altitude over the considered cells. We employ a swarm of at most 3 coordinated AVs, and 6 of AV s are interfering with the AV of interest. The location of the desired AV's serving BS and the HAP/LEO satellite projection on the ground is assumed at the origin. The horizontal distance of the HAP (LEO satellite) and its ground station is set as 5 (300) km. Altitude and number of LEO satellites in Table I are assumed based on Starlink constellation. In [45], the Rician K-factor was found to increase exponentially with elevation angle between two nodes. Here for simplicity, we assume that the Rician factor of each link increases linearly with the elevation angle. The elevation angles are considered from 0° to 90° with a 10° step, and the Rice factor is assumed to be constant in each interval. The experiments are provided to assess the reliability and network availability of different E2E paths and their parallel combinations for remote piloting of eVTOLs and investigate how we can achieve high E2E reliability and low E2E latency by MC along with adjusting system parameters such as data rate, bandwidth, CoMP cluster size, and interference level.

5.1.8 Simulation Results and Conclusions

Figure 26 (a) Reliability and (b) network availability performance of multi-path connectivity vs. data rate. shows the overall error probability and network unavailability of different multi-path connectivity with respect to the data rate when the AVs' allocated bandwidth, B^{xy}, xy $\in \{\mathrm{ga}, \mathrm{aa}, \mathrm{ha}, \mathrm{sa}\}$, is $0.8\ \mathrm{MHz}$. CoMP cluster size and probability of interference are set as 3 and 0.05, respectively. Figure 26 depicts the performance gain of multiple communication paths connectivity with DA2G/JT CoMP as a master connectivity.

It is observed that for the minimum required data rate of $250\ \mathrm{kbps}$, the reliability of "DA2G +3 -A2A" and "DA2G + Sat-S/Ka" schemes is ~ 0.99, and their network availability is ~ 0.97 and ~ 0.93, respectively, which shows improvement compared to the single RAT transmission.

Furthermore, "DA2G + HAP" and "DA2G $+3-\mathrm{A2\ A}+\mathrm{HAP}$ " schemes improve the target reliability of 0.99999 with network availability of ~ 0.999 up to $\sim 400\ \mathrm{kbps}$ and $\sim 500\ \mathrm{kbps}$ data rates, respectively. Additionally, it is shown that JT CoMP improves the reliability and network availability compared with DA2G communication because of combating the intercell interference by cooperation among ground BSs. The results show the cooperation of 3 adjacent ground BSs.

In Figure 27, we investigate how the CoMP cluster size affects the reliability and network availability, when data rate and AV's allocated bandwidth are $500\ \mathrm{kbps}$ and $0.8\ \mathrm{MHz}$, respectively, and $P_{\text{interf}} = 0.05$. As shown in Fig. 7, the reliability and availability can be improved by increasing CoMP cluster size. In this figure, CoMP cluster size of 1 is equivalent to DA2G communication. The performance gap between the cluster size of 1 and 2, i.e., adopting DA2G or JT CoMP, is notable, especially when A2A links via JT CoMP are considered as the auxiliary communication path, such as "CoMP + 3-A2A", "CoMP + 3-A2A + Sat-S/Ka", and "CoMP $+3-\mathrm{A2\ A}+\mathrm{HAP}$ " schemes.

Thus, utilizing JT CoMP along with A2A links and increasing CoMP cluster size can be a promising approach to achieve the target reliability and network availability. As it is observed, "CoMP $+3-\mathrm{A2\ A}$ + HAP" scheme with cluster size of at least 3 can achieve the required reliability in the evaluated scenario.

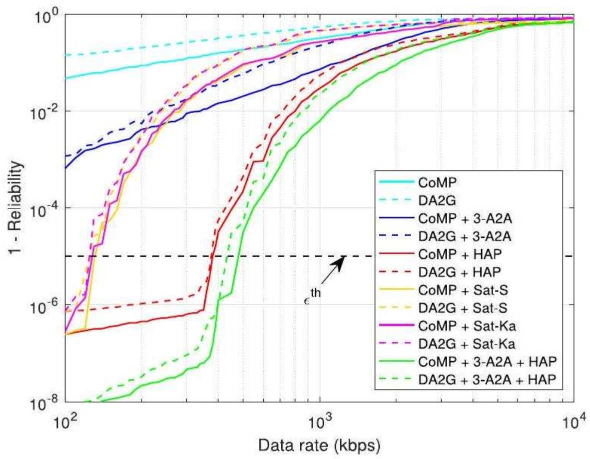

(a)

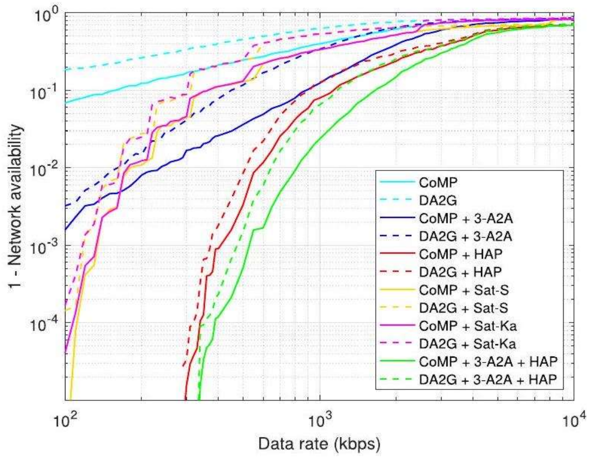

(b)

Figure 26 (a) Reliability and (b) network availability performance of multi-path connectivity vs. data rate.

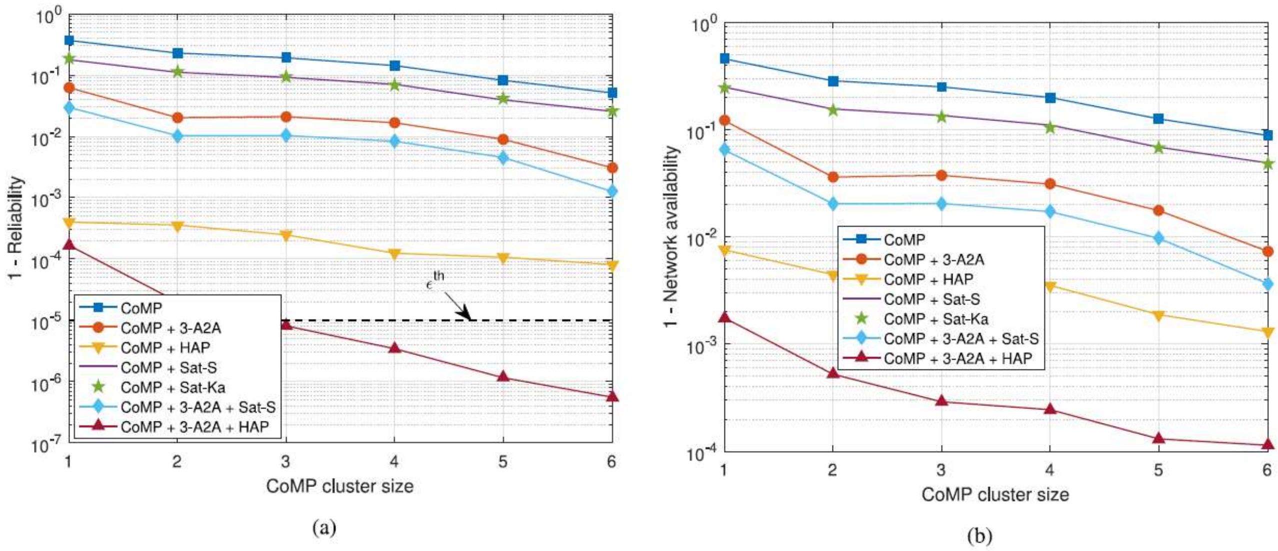

Figure 27(a) Reliability and (b) network availability performance vs. CoMP cluster size.

5.2 Free-Space Optics

Free-Space Optics (FSO) could be used as Inter Satellite Links (ISL), Inter HAPS Links and orbit-to-ground links (also called Direct To Earth (DTE).

Compared to the RF based ISL the main advantages of optical inter satellite links (OISL) are driven by a higher bandwidth, lower terminal SWaP, unlicensed spectrum (no ITU frequency coordination required), and minimized interference between densely packed constellations [48]. Typical requirements for OISL are 10 Gbps and more for 6000 km distance range.

5.2.1 Inter Satellite Links

As described in [49], ISLs are necessary to reduce the number of ground stations. Additionally, the ISLs are required to guarantee an ultra-secure communication and gateway independent meshed network data connectivity, from transmitter to receiver.

As minimum of four laser terminals per satellite are required to establish the intra-plane and inter-plane links between the satellites of one constellation. An example for ISLs is shown in the Figure 28. The SWaP of each terminal launched into orbit has a direct impact on the cost and the power needed by the satellite, which translates into the size of the solar panels, power harness, and battery storage [48].

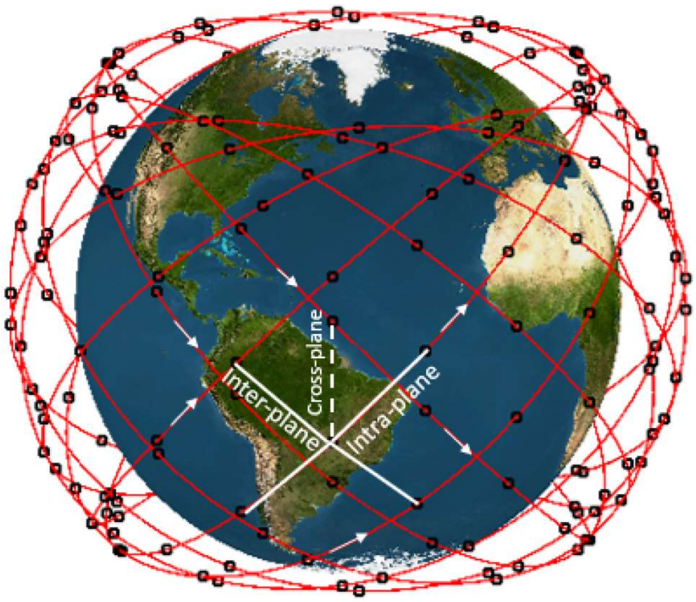

Figure 28 Walker orbit 192/12/45/2[6] highlighting the intra-plane, inter-plane, and cross-plane links between satellites [C. Carrizo, "Optical inter-satellite link terminals for next generation satellite constellations", 2020-03-02]

10 Gb/s and 7,000 km distance can be provided with the SCOT80 laser communication terminal developed by Tesat with a mass of 15 kg and a total power consumption of 80 W [50].

[6] 192 is the total number of satellites, 12 is the number of orbital planes, the constellation inclination is 45 degrees and 2 is the relative spacing between satellites in adjacent planes

Another example for an OISL flight terminal is CONDOR Mk3 by mynaric[7]. The block diagram in Figure 29 show that the data interface from the satellite processing unit to the electronics system of the OISL terminal is realized via 10 Gigabit Ethernet IEEE 802.3.

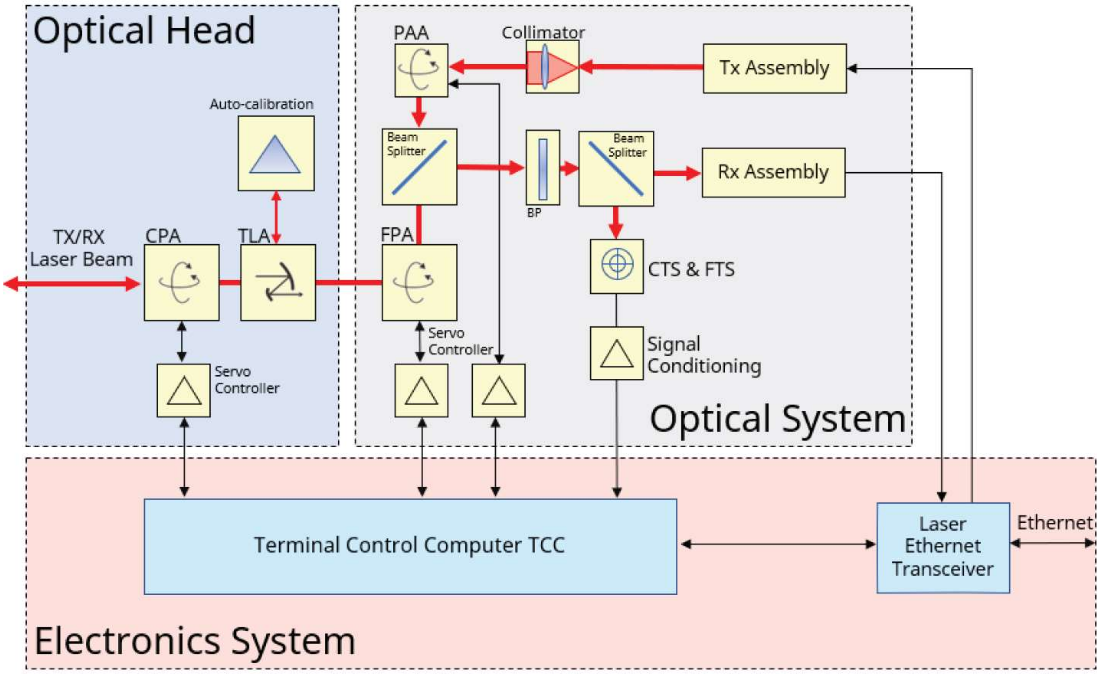

Figure 29 Functional block diagram of the CONDOR terminal [48]

A variant without Coarse Pointing Assembly (CPA), for body-pointing, can be used for intra-plane links, further reducing the weight of the terminal set (4 terminals) by 12 kg [48].

[7] https://mynaric.com/products/space/

Parameter	Nominal Value	
Aperture Diameter	Ø	80 mm
Operational Wavelength	λ	C-Band 1550 nm
Beam Divergence		17.44 μrad
Coarse Steering Range (customizable)	Azimuth	±175 deg
	Elevation	(+5, -25) deg
Fine Steering Range	Azimuth	± 0.35 deg
	Elevation	± 0.35 deg
Point-Ahead Steering Range		> ± 0.1 deg
Acquisition Field of View		± 0.125 deg
Acquisition Time	No Calib. / Calib.	< 30 sec / 2 sec
Alignment Stability		< 1 μrad
Tracking Stability		< 1 μrad
Data Rate	Per channel	10 Gbps
Dimensions	HxWxD	590 x 253 x 228 mm (w/CPA)
		345 x 253 x 167 mm (w/o CPA)
		345 x 312 x 80 mm (Electronics unit)
Mass		<18 kg
Input Voltage		28 V (DC)
Power Consumption		<60 W
Optical Tx Power		1 W
Communication Interfaces		802.3 IEEE standard
Operating Temperature	min./max.	-40° C / +60 ° C
Lifetime		7 or 10 years

Figure 30 CONDOR Gen1 terminal specification [48]

Figure 31 shows that the system can operate with a reduced data rate of 5 Gbit/s and 3 dB power margin at a maximum distance of 7780 km with the standard terminal configuration. Without the 3 dB margin a data rate of 10 Gbit/s is possible.

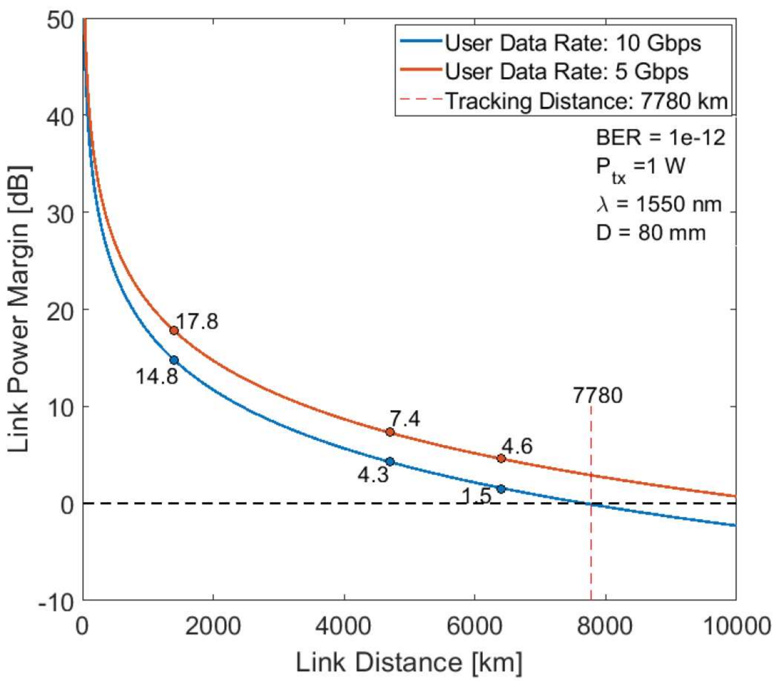

Figure 31 Link power margin for different data rates and link distances [48]

5.2.2 Inter HAPS Links

HAPS are defined by the International Telecommunications Union (ITU) as an aerial terminal that can stay at a quasi-stationary position in the stratosphere at an altitude of about 20 – 50 km [51]. As their position is quasi-stationary, the Doppler shift is decreased to a certain level that do not impact the communication performance. The precision and tracking problems can also be neglected due to the quasi-stationary position of HAPS systems.

In general, HAPS can be used as platforms for remote sensing, in sparsely populated areas with limited infrastructure, in case of natural disasters, for navigation and localization [52].

Inter-HAPS links could be used for services with minimal ground network infrastructure - for example, as back up if terrestrial networks are damaged by disasters [51] and major sporting events.

As the maximum cloud height of 13 km can be assumed [53], the optical paths above this altitude are not affected by the cloud blockage [52].

An optical communication terminal module, called SCOT80, developed by TESAT could be used for optical inter HAPS links [50].

5.2.3 Links between HAPS and Satellites

See inter satellite links in chapter 5.2.1 of [54].

5.2.4 Direct to Earth (DTE)

In general, DTE FSO are already operable but the cloud coverage, harsh weather conditions and atmospheric turbulence can limit communication considerably or make it completely impossible [52] [55]. Thus, the use of DTE FSO links is not suitable in all regions of the world.

European studies on the availability statistics of optical HAP-to-ground links show single-link availabilities ranging from 20% during winter in Northern Europe to over 70% during summer in Southern Europe [56].

Smaller communication terminals from TESAT for small satellites and Direct To Earth (DTE) connections are CUBE LCT (data rate up to 100 Mbps, power consumption 8 W and mass of 360 g) and TOSIRIS (data rate up to 10 Gbps, power consumption 40 W and mass of 8 kg) [57].

5.2.5 Overview of FSO Modules

Nr.	Module	Data rate [Gbit/s]	Range [km]	Power Consumption [W][8]	Mass [kg]	Application	Manufacturer
1	SCOT80	10	8000	60-86	15	LEO to LEO	TESAT
2	Smart LCT	1.8	45000	130	30	LEO to GEO	TESAT
3	LTC 135	1.8	80000	150	53	GEO to GEO, GEO to LEO, GEO to Airborne, GEO to Ground	TESAT
4	CUBE LTC	0.1	1500	8-10	0.397	LEO to Ground	TESAT
5	TOSIRIS	10	1500	40	8	LEO to Ground	TESAT
6	CONDOR Mk3	0.3-2.5	6500	-	-	LEO to LEO	mynaric
7	CONDOR Mk2	0.3-1.25	5000	-	-	LEO to LEO	mynaric
8	HAWK	7	12	110-150	13	Air to Air, Air to Ground	mynaric
9	LEOCAT	up to 10	4400	-	-	LEO	FSO Instruments

Table 23 Overview of FSO Modules.

6 Sustainability

The information and communications technologies (ICT) industry play an important role in today's digital economy and has enormous potential to improve people's lives by enabling and providing worldwide mobile connectivity and global coverage [58].

Combined airspace and non-terrestrial networks (combined ASN) supporting a 3D network architecture improves resilience of communication infrastructure and promotes digital innovation over large geographical areas. For example, reliable connectivity in rural areas enable activities that are key on improving sustainable development, such as smart agriculture and automation on environmental monitoring. These activities have the potential to improve management of natural resources and contribute to environmental sustainability [58].

7 Conclusion

A combined ASN having a 3D architecture can contain different communication links including air-to-air (A2A), air-to-ground (A2G), high altitude platforms stations (HAPS), and non-terrestrial networks (NTN) satellite link communications. This deliverable presented analysis of selected links within a 3D

[8] depending on data rate

architecture and describes best link parameters and antenna systems for these selected communication channels.

It is noted that a multitude of different bands can be considered for each link. We identified existing and envisioned spectrum candidates for several of the links. For example, a HAPS to terrestrial user link can already use 3GPP bands on sub-6GHz (FR1) for handset type of user equipment (UE). FR3 is a potential new spectrum candidate for this link, for which several studies exist, and which will be further covered in WRC-27.

We set target Key Performance Indicators (KPIs) values for the 6G time frame for selected links, aiming to set realistic figures which are technologically reachable by 6G systems. This is confirmed by analysis of the several links of a 3D architecture network. It is important to properly determined the required data rate of satellite feeder links, so that they do not become a bottleneck.

For HAPS with satellite backhaul, analysis of several antenna configurations has been performed. This analysis identified the antenna configuration bringing the best results for each orbit. For the case of HAPS serving terrestrial UEs, the link analysis concluded that throughput values meet the target values set for the 6G timeframe.

Analysis of the link between terrestrial base station (BS) and airborne UEs, such as unmanned aerial vehicles (UAVs) and electric vertical take-off and landing (eVTOL) flying taxis, concludes that target KPIs for 6G can be meet by using suitable antenna configuration, and large enough bandwidth.

We study how end-to-end connectivity requirements for remote piloting scenarios can be meet using multi connectivity. We show that these requirements are satisfied using multi connectivity, by considering vertical heterogeneous networks with direct air-to-ground (DA2G) and air-to-air (A2A) communication, high altitude platforms, and low Earth orbit (LEO) satellites. Thus, showing that multi connectivity is a key enabler for safe operation of aerial vehicles.

Finally, we explore the use of free-space optics (FSO) for use as Inter Satellite Links (ISL), Inter HAPS Links, links between satellite and HAPS, and orbit-to-ground links. An overview of FSO modules is presented highlighting aspects that make them suitable for each of the mentioned links.

References:

Chapter 1

1. "6G for Connected SKY," [Online]. Available: https://www.6g-sky.net/

Chapter 2

2. 6G-SKY D4.1 System architecture and network design aspects for NTN-based communication for terrestrial users, chapter 6

Chapter 3

3. ITU-R, "Minimum requirements related to technical performance for IMT-2020 radio interfaces," Report M.2410-0 (11/2017)
4. W. L. Stutzman, "Estimating directivity and gain of antennas," in IEEE Antennas and Propagation Magazine, 1998. available in https://doi.org/10.1109/74.730532

Chapter 4

5. A. R. Dastkhosh, Z. Khan, M. Naseh and F. Lin, "Link Budget Calculations for K/Ka-band Satellite Mobile Communication Systems," 2022 IEEE MTT-S International Wireless Symposium (IWS), Harbin, China, 2022.
6. 3GPP TR 38.876 "Air-to-Ground network for NR"
7. L. Nogueira Ribeiro, S. Hastürkoğlu and J. Grävendieck, "Ground Base Antenna Design for Air-to-Ground Communications," 2024 European Conference on Antennas and Propagation (EUCAP).
8. G. Fodor, S. Fodor and M. Telek, "MU-MIMO Receiver Design and Performance Analysis in Time-Varying Rayleigh Fading," in IEEE Transactions on Communications, vol. 70, no. 2, pp. 1214-1228, Feb. 2022, doi: 10.1109/TCOMM.2021.3126760.
9. S. Fodor, G. Fodor, D. Gürgünoğlu and M. Telek, "Optimizing Pilot Spacing in MU-MIMO Systems Operating Over Aging Channels," in IEEE Transactions on Communications, vol. 71, no. 6, pp. 3708-3720, June 2023, doi: 10.1109/TCOMM.2023.3261384.
10. J. V. Saraiva, R. P. Antonioli, G. Fodor, W. C. Freitas and Y. C. B. Silva, "A Distributed Game-Theoretic Solution for Power Management in the Uplink of Cell-Free Systems," 2022 IEEE Globecom Workshops (GC Wkshps), Rio de Janeiro, Brazil, 2022, pp. 1084-1089, doi: 10.1109/GCWkshps56602.2022.10008611.
11. M.C.R Lobão, W.d.O. Feitosa, R.P. Antonioli, Y.C.B. Silva, W.C. Freitas and G. Fodor, "On the Impact of Antenna Tilt on Cell-Free Systems Serving Ground Users and UAVs," 2023 XLI Brazilian symposium on telecommunications and signal processing (SBRT), 2023, doi: 10.14209/sbrt.2023.1570917523.
12. I. M. Braga, R. P. Antonioli, G. Fodor, Y. C. B. Silva and W. C. Freitas, "Decentralized Joint Pilot and Data Power Control Based on Deep Reinforcement Learning for the Uplink of Cell-Free Systems," in IEEE Transactions on Vehicular Technology, vol. 72, no. 1, pp. 957-972, Jan. 2023, doi: 10.1109/TVT.2022.3211908.
13. R. Delgado Pulgar, G. Fodor, H. Do and Z. T. Qi, "Performance Analysis of 5G Cellular Networks Serving Terrestrial and Aerial Users in the Presence of Interference Coupling," 2023

IEEE Conference on Standards for Communications and Networking (CSCN), Munich, Germany, 2023, pp. 118-123, doi: 10.1109/CSCN60443.2023.10453137.
14. H. Do, R. D. Pulgar, G. Fodor and Z. Qi, "Cellular Connectivity for Advanced Air Mobility: Use Cases and Beamforming Approaches," in IEEE Communications Standards Magazine, vol. 8, no. 1, pp. 65-71, March 2024, doi: 10.1109/MCOMSTD.0007.2200069.
15. https://www.itu.int/dms_pub/itu-r/opb/act/R-ACT-WRC.15-2023-PDF-E.pdf
16. Jorn Christensen, ITU Regulations for Ka-band Satellite Networks, AsiaSat
17. Argyrios Kyrgiazos, Barry Evans and Paul Thompson, High Throughput Satellite Gateway Feeder Link (Q/V/W bands), University of Surrey
18. Ka/Q/V—Band Gateway Antennas, https://d26wgh18tyxdzi.cloudfront.net/productResources/Ka-Q-V-Band-Gateway-Antennas_2022.pdf
19. 4.0M LEO/MEO GATEWAY TERMINALS, available in https://www.cpii.com/docs/datasheets/938/03-LEO-MEO%20Datasheet%20-%204.0m%20Gateway%20Terminals%20Datasheet%2012mar24.pdf
20. 9.2m LEO Earth Station Antenna, CALIAN, available in https://d26wgh18tyxdzi.cloudfront.net/productResources/9.2m-LEO-Earth-Station-Antenna.pdf
21. 13m Ka Band Antenna, CALIAN, available in https://d26wgh18tyxdzi.cloudfront.net/productResources/13m-Ka-Band-Antenna.pdf
22. System Architectures and Implementation Scenarios Document (SAID), Airbus Defence and Space GmbH, 5GIS-ADS-TN_3000_010m, 22 Juli 2022
23. Geordie George, Samhita Roy, Sahana Raghunandan, Christian Rohde and Thomas Heyn, "5G New Radio in Nonlinear Satellite Downlink: A Physical Layer Comparison with DVB-S2X", Fraunhofer IIS, 2021 IEEE 4th 5G World Forum (5GWF), available in https://ieeexplore.ieee.org/stamp/stamp.jsp?tp=&arnumber=9604976

Chapter 5

24. A. Baltaci, E. Dinc, M. Ozger, A. Alabbasi, C. Cavdar, and D. Schupke, "A survey of wireless networks for future aerial communications (FACOM)," IEEE Commun. Surveys Tuts., vol. 23, no. 4, pp. 2833–2884, 4th Quart., 2021.
25. P. Popovski et al., "Wireless access for ultra-reliable low-latency communication: Principles and building blocks," IEEE Netw., vol. 32, no. 2, pp. 16–23, Mar./Apr. 2018.
26. C. She, C. Yang, and T. Q. Quek, "Radio resource management for ultra-reliable and low-latency communications," IEEE Commun. Mag., vol. 55, no. 6, pp. 72–78, Jun. 2017.
27. J. J. Nielsen, R. Liu, and P. Popovski, "Ultra-reliable low latency communication using interface diversity," IEEE Trans. Commun., vol. 66, no. 3, pp. 1322–1334, Mar. 2018.
28. J. Thornton, D. Grace, M. H. Capstick, and T. C. Tozer, "Optimizing an array of antennas for cellular coverage from a high altitude platform," IEEE Trans. Wireless Commun, vol. 2, no. 3, pp. 484–492, May 2003.
29. F. Vatalaro, G. E. Corazza, C. Caini, and C. Ferrarelli, "Analysis of LEO, MEO, and GEO global mobile satellite systems in the presence of interference and fading," IEEE J. Sel. Areas Commun., vol. 13, no. 2, pp. 291–300, Feb. 1995.
30. N. Shlezinger, R. Fu, and Y. C. Eldar, "DeepSIC: Deep soft interference cancellation for multiuser MIMO detection," IEEE Trans. Wireless Commun, vol. 20, no. 2, pp. 1349–1362, Feb. 2021.

31. M. S. Sim, M. Chung, D. Kim, J. Chung, D. K. Kim, and C.-B. Chae, “Nonlinear self-interference cancellation for full-duplex radios: From link-level and system-level performance perspectives,” IEEE Commun. Mag., vol. 55, no. 9, pp. 158–167, Sep. 2017.
32. S. Xu, H. Wang, T. Chen, Q. Huang, and T. Peng, “Effective interference cancellation scheme for device-to-device communication underlaying cellular networks,” in Proc. IEEE VTC-Fall, 2010, pp. 1–5.
33. F. Salehi, M. Ozger and C. Cavdar, "Reliability and Delay Analysis of 3-Dimensional Networks With Multi-Connectivity: Satellite, HAPs, and Cellular Communications," in IEEE Transactions on Network and Service Management, vol. 21, no. 1, pp. 437-450, Feb. 2024.
34. C. She, C. Yang, and T. Q. Quek, “Joint uplink and downlink resource configuration for ultra-reliable and low-latency communications,” IEEE Trans. Commun., vol. 66, no. 5, pp. 2266–2280, May 2018.
35. R. Devassy et al., “Finite-blocklength analysis of the ARQ-protocol throughput over the Gaussian collision channel,” in Proc. IEEE ISCCSP, 2014, pp. 173–177.
36. Z. Mayer, J. Li, A. Papadogiannis, and T. Svensson, “On the impact of control channel reliability on coordinated multi-point transmission,” Wireless Commun. Netw., vol. 2014, no. 1, pp. 1–16, 2014.
37. K. Kwak, H. W. Je, S.-H. Park, and S. Choi, “CoMP joint transmission for Gaussian broadcast channels in delay-limited networks,” IEEE Trans. Veh. Technol., vol. 66, no. 3, pp. 2053–2058, Mar. 2017.
38. M. K. Karakayali, G. J. Foschini, and R. A. Valenzuela, “Network coordination for spectrally efficient communications in cellular systems,” IEEE Wireless Commun., vol. 13, no. 4, pp. 56–61, Aug. 2006.
39. D.-H. Jung, J.-G. Ryu, W.-J. Byun, and J. Choi, “Performance analysis of satellite communication system under the shadowed-Rician fading: A stochastic geometry approach,” IEEE Trans. Commun., vol. 70, no. 4, pp. 2707–2721, Apr. 2022.
40. F. Salehi, M. Ozger, N. Neda, and C. Cavdar, “Ultra-reliable lowlatency communication for aerial vehicles via multi-connectivity,” in Proc. EuCNC/6G Summit, 2022, pp. 166–171.
41. 3GPP, “Study on enhanced LTE support for aerial vehicles (release 15),” Sophia Antipolis, France, 3GPP Rep. TR 36.777, Dec. 2017.
42. I. Leyva-Mayorga et al., “LEO small-satellite constellations for 5G and beyond-5G communications,” IEEE Access, vol. 8, pp. 184955–184964, 2020.
43. M. M. Azari et al., “UAV-to-UAV communications in cellular networks,” IEEE Trans. Wireless Commun, vol. 19, no. 9, pp. 6130–6144, Sep. 2020.
44. C. She, Y. Duan, G. Zhao, T. Q. Quek, Y. Li, and B. Vucetic, “Crosslayer design for mission-critical IoT in mobile edge computing systems,” IEEE Internet Things J., vol. 6, no. 6, pp. 9360–9374, Dec. 2019.
45. M. M. Azari et al., “Optimal UAV positioning for terrestrial-aerial communication in presence of fading,” in Proc. IEEE GLOBECOM, 2016, pp. 1–7.
46. European Aviation Network, “World Leading Innovation Tailor[1]Made for Europe,” Accessed: 2021-01-20. [Online]. Available: https://www.wired.com/story/spacex-satellites-orbital-altitude/
47. 3GPP, “Study on New Radio (NR) to support non-terrestrial networks (Release 15),” TR 38.811, 3rd Generation Partnership Project, Tech. Rep., Sep. 2020.
48. C. Carrizo, “Optical inter-satellite link terminals for next generation satellite constellations”, 2020-03-02
49. I. del Portillo, B. G. Cameron, E. F. Crawley, “A Technical Comparison of Three Low Earth Orbit Satellite Constellation Systems to Provide Global Broadband”, 2018-10-01

50. SCOT80 Laser Communication Terminal for Satellite Networks, TESAT, https://www.tesat.de/images/tesat/products/220607_DataSheet_SCOT80_A4.pdf, last updated 2023-05-25
51. ITU, “HAPS – High-altitude platform systems”, https://www.itu.int/en/mediacentre/backgrounders/Pages/High-altitude-platform-systems.aspx , last update April 2022
52. Franz Fidler, Markus Knapek, Joachim Horwath, and Walter R. Leeb, “Optical Communications for High-Altitude Platforms”, IEEE JOURNAL OF SELECTED TOPICS IN QUANTUM ELECTRONICS, VOL. 16, NO. 5, SEPTEMBER/OCTOBER 2010
53. D. Giggenbach, R. Purvinskis, M. Werner, and M. Holzbock, “Stratospheric optical interplatform links for high altitude platforms,” presented at the 20th AIAA Int. Commun. Satellite Syst. Conf. Exhib., Montreal, QB, Canada, 2002
54. E. Erdogan, I. Altunbas, G. K. Kurt and H. Yanikomeroglu, "Cooperation in Space: HAPS-Aided Optical Inter-Satellite Connectivity With Opportunistic Scheduling," in IEEE Communications Letters, vol. 26, no. 4, pp. 882-886, April 2022, doi: 10.1109/LCOMM.2022.3140247.
55. M. Knapek, J. Horwath, F. Moll, B. Epple, N. Courville, H. Bischl, and D. Giggenbach, “Optical high-capacity satellite downlinks via high altitude platform relays,” in Proc. SPIE Free-Space Laser Commun. VII, vol. 6709, pp. 6709E-1–6709E-12, 2007
56. F. Moll and M. Knapek, “Wavelength selection criteria and link availability due to cloud coverage statistics and attenuation affecting satellite, aerial, and downlink scenarios” SPIE Free-Space Laser Commun. VII, vol. 6709, pp. 670916-1–670916-12, 2007.
57. TESAT, Laser Products, https://www.tesat.de/products, last updated 2023-05-25

Chapter 6

58. https://www.itu.int/en/sustainable-world/Pages/default.aspx

Figures:

Tables:

8 Annexes

8.1 Target KPI worksheets

Detailed KPI targets for the 5G and 6G timeframes are available in the Figures between Figure 32 and Figure 35.

In these figures the following link definitions are used:

- HAPS_GEO: link between HAPS and GEO
- HAPS_MEO: Link between HAPS and MEO
- HAPS_LEO: Link between HAPS and LEO
- HAPS_HAPS: Link connecting two HAPS
- GS_GEO: Link between Ground Station (GS) and GEO
- GS_LEO: Link between GS and LEO
- HAPS_UE_Terr: Link between HAPS and terrestrial UEs
- Terr BS_UAV, eVTOL, Helicopter: Link between a terrestrial Base station and aerial UE, like UAV, eVTOL, and Helicopter
- AC_SAT: Link between Aircraft and Satellite
- AC_Terr BS: Link between Aircraft and terrestrial BS
- AC_Terr BS Airport: Link between Aircraft and terrestrial BS located at Airport
- Passenger: Requirements for a passenger/crew inside aircraft

	HAPS_GEO	HAPS_MEO	HAPS_LEO	HAPS_HAPS	GS_GEO	GS_LEO
Peak data rate (user terminated or DL)	260 Mbps	240 Mbps	210Mbps	n/a	0.5 Gbit/s	32Mbit/s ... 212Mbit/s
Peak data rate (user terminated or UL)	150 Mbps	190 Mbps	210Mbps	n/a	2 Gbit/s	1.2Gbit/s ... 7.42Gbit/s
Experienced user thoughput (user terminated or DL)	260 Mbps	240 Mbps	210Mbps	n/a		-
Experienced user thoughput (user originated or UL)	150 Mbps	190 Mbps	210Mbps	n/a		-
Beam/cell capacity DL	1444 Mbps	1333 Mbps	1167Mbps	n/a		32Mbit/s ... 212Mbit/s
Beam/cell capacity UL	833 Mbps	1055 Mbps	1167Mbps	n/a		1.2Gbit/s ... 7.42Gbit/s
Total number of Beams/cells DL	500	16	16	n/a	1-8	1-4
Total number of Beams/cells UL	500	16	16	n/a	1-8	1-4
5th percentile spectral efficiency DL				n/a		-
5th percentile spectral efficiency UL		1333.333333		n/a		-
traffic capacity (DL)				10 Gbps		-
traffic capacity (UL)				10 Gbps		-
Minimum elevation angle	30°	30°	30°	n/a	-	
Acquisition time	5s to 60s	60s	60s	n/a	-	
Reliability/Availability (%)				99.9	99.9	99.9
User density				n/a	1-2	
mobility				< 500 km/h	-	-
UE type	6MHz, Ka band	6MHz, Ka band	6MHz, Ka band	n/a		
Max EIRP	49 dBW	49 dBW	49 dBW	n/a	55dBW	
G/T	11.2 dBi	11.2 dBi	11.2 dBi	n/a	36dB/K	
Polarization	RHCP/LHCP	RHCP/LHCP	RHCP/LHCP	n/a	circular	circular
Location (geographic location)				Global		
Height considerations				>14 km		
End to end latency	142ms	37ms	7ms	< 600 km	541.46 ms (max.), 477.48 ms (min.) (Note 1)	
C-plane latency				10 ms		40 ms
U-plane latency				n/a		10 ms
Source / Reference (e.g. 3GPP TS)				n/a		ITU-R M.2514-0, 3GPP TSG RAN WG1 #116
Notes/ Comments				n/a	Note 1: 3GPP TR 38.811	https://www.itu.int/dms_pub/itu-r/opb/rep/R-REP-M.2514-2022-PDF-E.pdf

Figure 32 Technical performance requirements in 5G time frame for selected HAPS and satellite links

	HAPS_GEO	HAPS_MEO	HAPS_LEO	HAPS_HAPS	GS_GEO	GS_LEO
Peak data rate (user terminated or DL)	790 Mbps	740 Mbps	660Mbps	n/a	2 Gbit/s	1.06 Gbit/S
Peak data rate (user terminated or UL)	325 Mbps	440 Mbps	510Mbps	n/a	8 Gbit/s	37.1 Gbit/s
Experienced user thoughput (user terminated or DL)	790 Mbps	740 Mbps	660Mbps	n/a		-
Experienced user thoughput (user originated or UL)	325 Mbps	440 Mbps	510Mbps	n/a		-
Beam/cell capacity DL	1462 Mbps	1370 Mbps	1222Mbps	n/a		1.06 Gbit/S
Beam/cell capacity UL	602 Mbps	814 Mbps	944Mbps	n/a		37.1 Gbit/s
Total number of Beams/cells DL	1000	100	100	n/a	1-8	1-4
Total number of Beams/cells UL	1000	100	100	n/a	1-8	1-4
5th percentile spectral efficiency DL				n/a		-
5th percentile spectral efficiency UL		0		n/a		-
traffic capacity (DL)				100 Gbps		-
traffic capacity (UL)				100 Gbps		-
Minimum elevation angle	30°	30°	30°	n/a	-	
Acquisition time	2s to 20s	20s	30s	n/a	-	
Reliability/Availability (%)				99.99	99.99	99.99
User density				n/a	1-4	
mobility				< 500 km/h	-	-
UE type	VSAT (25W BUC), BW = 108MHz, Ka band	VSAT (25W BUC), BW = 108MHz, Ka band	VSAT (25W BUC), BW = 108MHz, Ka band	n/a		
Max EIRP	49.4 dBW	49.4 dBW	49.4 dBW	n/a	0	
G/T	11.6 dBi	11.6 dBi	11.6 dBi	n/a	0	
Polarization	RHCP/LHCP	RHCP/LHCP	RHCP/LHCP	n/a	circular	circular
Location (geographic location)				Global		
Height considerations				>14 km		
End to end latency	142ms	37ms	7ms	< 600 km	Transparent: 541.46 ms (max.), 477.48 ms (min.) (Note 1) Regenerative: 270.73 ms (max.), 238.74 ms (min.) (Note 1)	
C-plane latency				1 ms		
U-plane latency				n/a		
Source / Reference (e.g. 3GPP TS)				n/a		
Notes/ Comments				n/a	Note 1: 3GPP TR 38.811	

Figure 33 Technical performance requirements in 6G time frame for selected HAPS and satellite links

	HAPS_UE_Terr		Terr BS_UAV, eVTOL, Helicopter	
	5G timeframe	6G timeframe	5G timeframe	6G timeframe
Peak data rate (user terminated or DL)	200 Mbps	1000Mbps		
Peak data rate (user originated or UL)	50 Mbps	100Mbps		
Experienced user thoughput (user terminated or DL)	100Mbps	500Mbps	15 Mbit/s	50 Mbit/s
Experienced user thoughput (user originated or UL)	25 Mbps	50Mbps	7.5 Mbit/s	25 Mbit/s
Beam/cell capacity DL	200 Mbps	1000Mbps		
Beam/cell capacity UL	50 Mbps	250Mbps		
Total number of Beams (cells) DL	<20	91		
Total number of Beams (cells) UL	<20	91		
5th percentile spectral efficiency DL	2	4		
5th percentile spectral efficiency UL	0.5	1		
traffic capacity (DL)	200 Mbps	25Gbps	50 Mbit/s/aircraft (Note 1)	100 Mbit/s/aircraft (Note 1)
traffic capacity (UL)	100 Mbps	10Gbps	25 Mbit/s/aircraft (Note 2)	120 Mbit/s/aircraft (Note 2)
Minimum elevation angle	45	20		
Acquisition time	n/a	n/a		
Reliability/Availability (%)	99.9	99.99	0.999	0.999
Throughput per km2	0.7	3		
mobility	300 km/h	500 km/h	up to 500 km/h (Note 3)	up to 500 km/h (Note 3)
UE type	Smartphone type UE	Smartphone type UE	aircraft mounted	aircraft mounted
MIMO mode	1Tx4R	2Tx8R		
Max TX power	23 dBm	26 dBm		
Antenna gain	0 dBi	12 dBi		
Polarization	linear	linear		
xNB type	gNB			
MIMO mode	2 (DL), 1 (UL)	2 (DL), 2 (UL)		
Max TX power	10 W	100 W		
Antenna gain	28 dBi	38 dBi		
Polarization	Linear	Linear		
BW	20MHz	100MHz		
Location (geographic location)	Europe	Europe		
Height considerations	14...20 km	14...20 km		
End to end latency	20 ms	10 ms	100 ms UL / 20 ms DL (Note 4)	100 ms UL / 20 ms DL (Note 4)
Source / Reference (e.g. 3GPP TS)	DT 5G HAPS Experiments	n/a		
Notes/ Comments	HAPS Experiments using 5G over 20MHz channel BW on B7, FDD.		Note 1: Enough for up to 3 active UEs at 15 Mbit/s each plus 5 Mbit/s for aircraft data payload. Note 2: Either up to 3 active users at (7.5 Mbit/s) or use the 25 Mbit/s for remote UAV controller with HD video. Note 3: EASA eVTOL certification is valid for speeds up to 250 knots calibrated air speed (KCAS) approx 463 Km/h Note 4: From the remote UAV controller with HD video use case in 3GPP TS 22.125.Aim to get at least rural eMBB in 5G specs ITU M.2410	Note 1: Enough for 2 active UEs at 50 Mbit/s each. Note 2: Either, 2 active users at 25 Mbit/s each plus 50 Mbit/s for video or use the 120 Mbit/s for laser mapping/HD patrol. Note 3: EASA eVTOL certification up to 250 knots calibrated air speed (KCAS) approx 463 Km/h Note 4: From the remote UAV controller with HD video use case in 3GPP TS 22.125.Aim to get at least rural eMBB in 5G specs ITU M.2410.

Figure 34 Technical performance requirements in 5G and 6G time frames HAPS - Terrestrial UE link and the link between terrestrial BS and aerial UEs

	AC_SAT	AC_Terr BS	AC_Terr BS Airport	Passenger
Experienced user thoughput (user terminated or DL)	1200 Mbit/s	1200 Mbit/s	200 Mbit/s	50 Mbit/s
Experienced user thoughput (user originated or UL)	600 Mbit/s	600 Mbit/s	300 Mbit/s	30 Mbit/s
mobility	up to 1300km/h	up to 1300km/h	up to 500km/h	
UE type	aircraft mounted	aircraft mounted	aircraft mounted	Passenger/Crew/... BYOD, MTC
Location (geographic location)	moving	moving	moving within 20km airport radius	moving within cabin
Height considerations	0 to 12000m	0 to 12000m	0 to 1500m	(0 to 13000m)

Figure 35 KPIs in 6G time frame for selected links to aircraft

8.2 Link budget worksheets for GEO/MEO/LEO - HAPS link

Detailed link budget calculations are presented in the following tables.

ID	generation	orbit type	orbit height [km]	maximal distance [km]	max latency [ms]	link type	antenna 1	EIRP [dBW]	anntenna 2	G/T [dB/K]	frequency [GHz]	bandwidth [MHz]	atomspheric losses [dB]	implementation penalty [dB]	CNR [dB]	channel capacity [Mb/s]
1	5G	GEO	35786	38608.88	141.664	UL	A	49	GEO UL antenna	29.1	30	36	2	3	12.4122	151.3345
1	5G	GEO	35786	38608.88	141.664	DL	GEO DL antenna	72.663	A	11.2	20	36	2	3	21.697	259.8238
2	5G	GEO	35786	38608.88	141.664	UL	B	37.7	GEO UL antenna	29.1	30	36	2	3	1.1122	43.0749
2	5G	GEO	35786	38608.88	141.664	DL	GEO DL antenna	72.663	B	5.2	20	36	2	3	15.697	189.1003
3	5G	GEO	35786	38608.88	141.664	UL	C	42.7	GEO UL antenna	29.1	30	36	2	3	6.1122	84.4675
3	5G	GEO	35786	38608.88	141.664	DL	GEO DL antenna	72.663	C	5.2	20	36	2	3	15.697	189.1003
4	5G	MEO	8000	10084.14	37.0008	UL	A	49	MEO UL antenna	21.1	30	36	2	3	16.0732	193.4851
4	5G	MEO	8000	10084.14	37.0008	DL	MEO DL antenna	59.663	A	11.2	20	36	2	3	20.358	243.9362
5	5G	MEO	8000	10084.14	37.0008	UL	B	37.7	MEO UL antenna	21.1	30	36	2	3	4.7732	72.0174
5	5G	MEO	8000	10084.14	37.0008	DL	MEO DL antenna	59.663	B	5.2	20	36	2	3	14.358	173.5765
6	5G	LEO	1200	1998.881	7.3343	UL	A	49	LEO UL antenna	9.1	30	36	2	3	18.1302	217.6106
6	5G	LEO	1200	1998.881	7.3343	DL	LEO DL antenna	43.163	A	11.2	20	36	2	3	17.915	215.0776
7	5G	LEO	1200	1998.881	7.3343	UL	B	37.7	LEO UL antenna	9.1	30	36	2	3	6.8302	91.4739
7	5G	LEO	1200	1998.881	7.3343	DL	LEO DL antenna	43.163	B	5.2	20	36	2	3	11.915	145.7299
8	5G	LEO	600	1075.088	3.9447	UL	A	49	LEO UL antenna	9.1	30	36	2	3	23.517	281.4696
8	5G	LEO	600	1075.088	3.9447	DL	LEO DL antenna	37.163	A	11.2	20	36	2	3	17.3019	207.8702
9	5G	LEO	600	1075.088	3.9447	UL	B	37.7	LEO UL antenna	9.1	30	36	2	3	12.217	149.1303
9	5G	LEO	600	1075.088	3.9447	DL	LEO DL antenna	37.163	B	5.2	20	36	2	3	11.3019	138.8713
10	5G	LEO	300	564.168	2.07	UL	A	49	LEO UL antenna	3	30	36	2	3	23.0178	275.5266
10	5G	LEO	300	564.168	2.07	DL	LEO DL antenna	31.063	A	11.2	20	36	2	3	16.8026	202.0147
11	5G	LEO	300	564.168	2.07	UL	B	42.7	LEO UL antenna	3	30	36	2	3	16.7178	201.021
11	5G	LEO	300	564.168	2.07	DL	LEO DL antenna	31.063	B	5.2	20	36	2	3	10.8026	133.335

Table 24 Analysis LEO/MEO/GEO links for 5G timeframe

ID	generation	orbit type	orbit height [km]	maximal distance [km]	max latency [ms]	link type	antenna 1	EIRP [dBW]	antenna 2	G/T [dB/K]	frequency [GHz]	bandwidth [MHz]	atomspheric losses [dB]	implementation penalty [dB]	CNR [dB]	channel capacity [Mb/s]
1	6G	GEO	35786	38608.88	141.664	UL	A 6G	49.4139	GEO UL antenna 6G	29.5	30	108	2	3	8.4688	324.5604
1	6G	GEO	35786	38608.88	141.664	DL	GEO DL antenna 6G	77.4342	A 6G	11.6	20	108	2	3	22.111	794.2264
2	6G	GEO	35786	38608.88	141.664	UL	B 6G	38.1139	GEO UL antenna 6G	29.5	30	108	2	3	-2.8312	65.3477
2	6G	GEO	35786	38608.88	141.664	DL	GEO DL antenna 6G	77.4342	B 6G	5.61	20	108	2	3	16.111	581.7792
3	6G	GEO	35786	38608.88	141.664	UL	C 6G	43.1139	GEO UL antenna 6G	29.5	30	108	2	3	2.1688	151.7129
3	6G	GEO	35786	38608.88	141.664	DL	GEO DL antenna 6G	77.4342	C 6G	5.61	20	108	2	3	16.111	581.7792
4	6G	MEO	8000	10084.14	37.0008	UL	A 6G	49.4139	MEO UL antenna 6G	21.5	30	108	2	3	12.1298	444.4392
4	6G	MEO	8000	10084.14	37.0008	DL	MEO DL antenna 6G	64.4342	A 6G	11.6	20	108	2	3	20.7719	746.5297
5	6G	MEO	8000	10084.14	37.0008	UL	B 6G	38.1139	MEO UL antenna 6G	21.5	30	108	2	3	0.82979	123.5951
5	6G	MEO	8000	10084.14	37.0008	DL	MEO DL antenna 6G	64.4342	B 6G	5.61	20	108	2	3	14.7719	535.078
6	6G	LEO	1200	1998.881	7.3343	UL	A 6G	49.4139	LEO UL antenna 6G	9.51	30	108	2	3	14.1868	514.8097
6	6G	LEO	1200	1998.881	7.3343	DL	LEO DL antenna 6G	47.9342	A 6G	11.6	20	108	2	3	18.329	659.8577
7	6G	LEO	1200	1998.881	7.3343	UL	B 6G	38.1139	LEO UL antenna 6G	9.51	30	108	2	3	2.8868	168.2369
7	6G	LEO	1200	1998.881	7.3343	DL	LEO DL antenna 6G	47.9342	B 6G	5.61	20	108	2	3	12.329	451.1814
8	6G	LEO	600	1075.088	3.9447	UL	A 6G	49.4139	LEO UL antenna 6G	9.51	30	108	2	3	19.5737	703.9512
8	6G	LEO	600	1075.088	3.9447	DL	LEO DL antenna 6G	41.9342	A 6G	11.6	20	108	2	3	17.7158	638.2019
9	6G	LEO	600	1075.088	3.9447	UL	B 6G	38.1139	LEO UL antenna 6G	9.51	30	108	2	3	8.2737	318.4488
9	6G	LEO	600	1075.088	3.9447	DL	LEO DL antenna 6G	41.9342	B 6G	5.61	20	108	2	3	11.7158	430.484
10	6G	LEO	300	564.168	2.07	UL	A 6G	49.4139	LEO UL antenna 6G	3.41	30	108	2	3	19.0744	686.2453
10	6G	LEO	300	564.168	2.07	DL	LEO DL antenna 6G	35.8342	A 6G	11.6	20	108	2	3	17.2165	620.6046
11	6G	LEO	300	564.168	2.07	UL	B 6G	43.1139	LEO UL antenna 6G	3.41	30	108	2	3	12.7744	466.3206
11	6G	LEO	300	564.168	2.07	DL	LEO DL antenna 6G	35.8342	B 6G	5.61	20	108	2	3	11.2165	413.7646

Table 25 Analysis LEO/MEO/GEO links for 6G timeframe

8.3 Link budget worksheets for HAPS - UE link

	HAPS - UE | Downlink			6G timeframe		5G timeframe	
				Scenario 1; HAPS Nadir position	Scenario 2; Service area edge position	Scenario 1; HAPS Nadir position	Scenario 2; Service area edge position
Transmitter	Freq	Link Budget Frequency	GHz	8.0	8.0	2.6	2.6
	BW	Total Bandwidth	MHz	**100**	**100**	**20**	**20**
	BSTxPwr	Total Transmit Power available per Transmit channel	W	**1.55**	**1.55**	**10**	**10**
	BSTxPwr	Total Transmit Power available per Transmit channel	dBm	31.9	31.9	40.0	40.0
	TxChanNo	Number of TX channels	-	**128**	**128**	**2**	**2**
	DLLayers	Nunber of DL layers	-	**2**	**2**	**2**	**2**
	BSTxPwrRE	TX power per Resource Element	dBm	17.9	17.9	12.0	12.0
	LFeeder	Tx_FeederLoss (distribution loss)	dB	0.5	0.5	0.5	0.5
	TxAntGain	Tx Antenna Gain	dBi	37.7	33.0	28.1	23.4
	EIRPRE	EIRP per RE	dBm	**55.1**	**50.4**	**39.6**	**34.9**
	EIRP	Total EIRP	dBm	**90.2**	**85.5**	**70.6**	**65.9**
Link Path	Dist	Link Distance	km	18.3	63.0	18.3	63.0
	FSPL	FSPL	dB	135.8	146.5	126.0	136.7
	LAtmGas	Atmospheric Gases and Water Vapor Attenuation	dB	0.1	0.9	0.1	0.5
	LRain	Rain Attenuation (ITU P.838-3, 10mm/h)	dB	0.1	2.6	0.1	0.2
	Fading	Fading Margin	dB	10.0	10.0	10.0	10.0
	PLTotal	Path Loss Total	dB	**146.0**	**159.9**	**136.2**	**147.4**
Receiver	RxAntGain	Rx Antenna Gain	dBi	12.5	9.1	0	0
	LBody	Body Loss	dB	3.0	3.0	3.0	3.0
	RxDivGain	Receiver Diversity Gain	dB	3.0	3.0	3.0	3.0
	RxLev	RxLev at Receiver Input	dBm	**-78.4**	**-100.5**	**-96.7**	**-112.5**
	SCBW	Subcarrier BW (OFDM SCS)	kHz	30	30	15	15
	SysTemp	System Temperature	K	290	290	290	290
	RxNF	Rx LNA NF	dB	8	8	8	8
	RxNfloor	Receiver Noise Floor	dBm	-121.2	-121.2	-124.2	-124.2
	Interference	Interference Margin	dB	1.0	1.0	3.0	3.0
	SEfactor	Spectrum efficiency increase factor	-	1.20	1.20	1.00	1.00
	SNR	SNR	dB	**41.8**	**19.7**	**24.6**	**8.7**
	Thput	Throughput (5G NR based)	**Mbps**	**1251.0**	**813.5**	**161.0**	**74.6**

Table 26 Link Budget DL

DL Throughput calculations are based on 3GPP TS 38.214, Section 5.1.3.2

MCS Index I_{MCS}	Modulation Order Q_m	Target code Rate x [1024] R	Spectral efficiency
0	2	120	0.2344
1	2	193	0.377
2	2	308	0.6016
3	2	449	0.877
4	2	602	1.1758
5	4	378	1.4766
6	4	434	1.6953
7	4	490	1.9141
8	4	553	2.1602
9	4	616	2.4063
10	4	658	2.5703
11	6	466	2.7305
12	6	517	3.0293
13	6	567	3.3223
14	6	616	3.6094
15	6	666	3.9023
16	6	719	4.2129
17	6	772	4.5234
18	6	822	4.8164
19	6	873	5.1152
20	8	682.5	5.332
21	8	711	5.5547
22	8	754	5.8906
23	8	797	6.2266
24	8	841	6.5703
25	8	885	6.9141
26	8	916.5	7.1602
27	8	948	7.4063
28	2	reserved	reserved
29	4	reserved	reserved
30	6	reserved	reserved
31	8	reserved	reserved

Table 27 3GPP TS 38.214 Table 5.1.3.1-2: MCS index table 2 for PDSCH and PUSCH

SINR [dB]	MCS [-]
-2	0.4
-1	1.7
0	3.0
1	4.2
2	5.3
3	6.3
4	7.3
5	8.2
6	9.0
7	9.8
8	10.6
9	11.3
10	12.0
11	12.6
12	13.3
13	13.9
14	14.5
15	15.1
16	15.8
17	16.4
18	17.0
19	17.7
20	18.4
21	19.1
22	19.9
23	20.7
24	21.6
25	22.5
26	23.5
27	24.5
28	25.7
29	26.9
30	28.2

Table 28 DL SINR and MCS based on HAPS experimental data

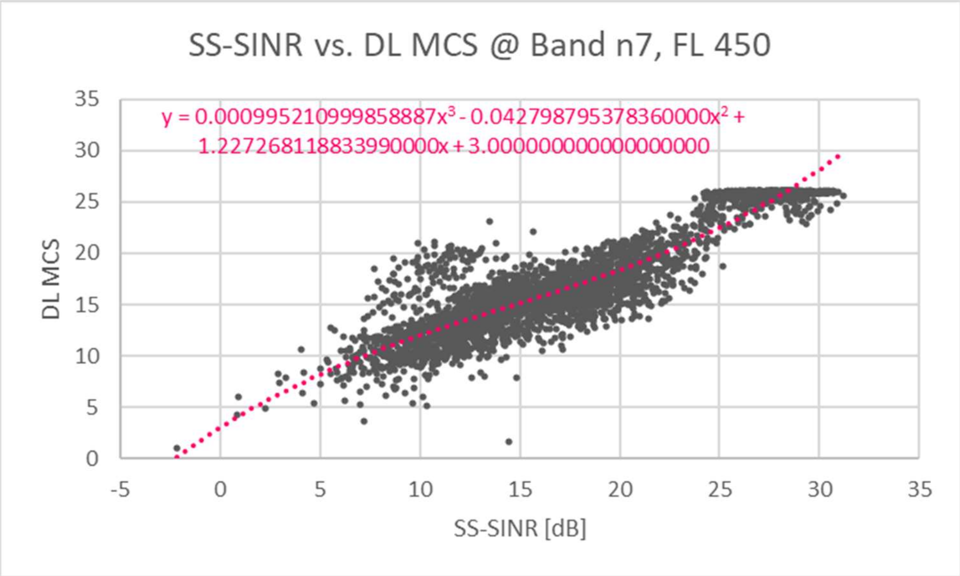

Figure 36 SINR vs DL MCS based on HAPS experimental data

For Uplink throughput estimation, two different sets of log files from field experiments are used for mapping between CL and SNR to UL throughput. These are summarized in Table 29 and Table 30 below. The 100 MHz normalized bandwidth is considered as FDD system, while n78 90 MHz system is TDD (using TDD pattern DDDSU).

5G TN, n7, 4T4R, 20MHz	
UL SINR	MovMed RLC UL
-38	0.8446
-36	1.0868
-30	1.1894
-26	1.2920
-24	1.4906
-21	1.6891
-20	2.0967
-18	2.5042
-17	2.9612
-16	3.4181
-15	3.1896
-14	3.9459
-13	4.7722
-12	5.6214
-11	6.8244
-10	8.8398
-9	10.8268
-8	11.1861
-7	11.6064
-6	14.6174
-5	18.4994
-4	22.8879
-3	25.5265
-2	31.7846
-1	34.4816
0	36.9378
1	39.2562
2	41.3478
3	42.4496
4	44.2590
5	46.6575
6	48.8109
7	50.9394
8	54.1625
9	56.7388
10	57.3606
11	58.4139
12	63.5936
13	68.3506
14	73.7355
15	76.6831
16	80.1238
17	85.2394
18	87.0796
19	87.5547
20	87.7124
21	87.7183
22	87.7762

5G TN, n78, 8T8R, 90MHz		Normalized@100MHz BW
UL SINR	MovMed RLC UL	MovMed RLC UL
29	62.7	303.1
27	62.7	303.1
26	62.3	301.0
25	61.7	298.1
24	60.9	294.3
23	60.7	293.1
22	60.3	291.1
21	59.8	288.7
20	56.8	274.6
19	56.1	271.2
18	55.4	267.7
17	53.8	260.0
16	51.7	249.7
15	48.6	234.8
14	46.0	222.3
13	45.2	218.2
12	44.0	212.3
11	39.0	188.3
10	33.5	162.0
9	27.7	133.7
8	22.9	110.6
7	20.1	96.9
6	19.1	92.4
5	18.7	90.3
4	18.7	90.5
3	18.5	89.2
2	16.0	77.3
1	10.0	48.3
0	10.4	50.0
-1	7.6	36.8
-2	5.3	25.8
-3	3.2	15.6
-4	2.1	10.1
-5	1.7	8.0
-6	1.0	4.9
-7	0.8	3.7
-8	0.7	3.3
-11	0.7	3.2
-12	0.6	2.9
-13	0.5	2.3
-14	0.4	1.7
-15	0.3	1.4
-17	0.2	1.0
-19	0.2	1.0
-23	0.2	0.9
-26	0.2	0.9
-29	0.2	0.9

Table 29 UL Throughput based on UL SINR

5G TN, n7, 4T4R, 20MHz	
CouplingLoss	MovMed RLC UL
90	87.91
91	87.91
92	87.91
93	87.91
94	87.75
95	87.36
96	86.55
97	84.89
98	81.39
99	79.29
100	76.68
101	73.98
102	69.74
103	64.96
104	60.07
105	58.58
106	57.41
107	56.84
108	56.23
109	55.55
110	52.05
111	49.06
112	47.12
113	45.13
114	43.27
115	42.08
116	40.78
117	39.21
118	37.27
119	34.27
120	30.91
121	25.07
122	24.03
123	20.70
124	15.26
125	11.64
126	11.32
127	10.87
128	8.98
129	6.80
130	6.12
131	4.54
132	4.27
133	3.32
135	2.63
136	2.13
138	1.76
140	1.72
143	1.69
145	1.49
146	1.29
148	1.19
154	1.09
157	0.84

5G TN, n78, 8T8R, 90MHz		Normalized@100MHz BW
CouplingLoss	MovMed RLC UL	MovMed RLC UL
82	62.7	303.1
84	62.7	303.1
88	62.7	303.1
89	62.1	300.0
90	61.4	296.5
91	60.8	293.7
92	60.4	291.6
93	60.0	289.9
94	57.4	277.5
96	56.1	270.8
97	54.4	262.6
98	52.0	251.3
99	49.1	237.2
100	46.4	224.2
101	45.2	218.3
102	44.3	213.9
103	40.6	196.3
104	36.5	176.1
105	32.0	154.8
106	25.6	123.9
107	20.6	99.8
108	19.5	94.4
109	18.6	89.9
110	18.8	90.8
111	18.9	91.2
112	17.4	84.1
113	14.0	67.8
114	10.3	49.7
115	11.9	57.6
116	8.0	38.4
117	5.1	24.8
118	3.5	17.0
119	2.4	11.5
120	1.8	8.6
121	1.1	5.1
122	0.8	3.9
123	0.8	3.8
127	0.7	3.5
128	0.6	2.9
129	0.4	2.1
131	0.4	1.7
132	0.2	1.2
134	0.2	1.0
139	0.2	1.0
141	0.2	0.9

Table 30 UL Throughput based on Coupling Loss

8.4 Link budget worksheets for Base station - airborne UE

The following tables present more details on the calculations for the link between terrestrial base station and airborne UEs.

Parameter	Symbol	Unit	5G	6G UAV	6G eVTOL
System parameters:					
Carrier frequency	Freq	GHz	3.5	10	10
Channel Bandwidth	BW	MHz	20.0	100.0	100.0
UL Bandwidth used for calculations	BWeff	MHz	18.4	98.3	98.3
Transmitter side:					
Transmit power	P_out	dBm	23.0	23.0	26.0
Pointing losses	L_pointingTX	dB	1.0	3.0	2.0
Path:					
Total TX to RX distance		m	1525.0	1525.0	3154.5
Path loss	PL	dB	110.0	119.1	125.4
Atmospheric loss	L_atmos	dB	0.4	1.2	1.5
Rain and water evaporation attenuation	L_rain	dB	0.0	0.3	0.7
shadowing/fading margin		dB	3.0	3.0	3.0
Total path loss	PL_total	dB	110.4	120.7	127.6
Receiver side:					
Antenna Gain	G_RX	dBi	24.2	33.8	33.8
Cable loss, line loss, and switch losses	L_implementationRX	dB	2.0	2.0	2.0
Receive noise factor	NF	dB	5.0	7.0	7.0
Metrics:					
Effective Isotropically Radiated Power	EIRP	dBm	22.0	20.0	24.0
Received signal power	S_RX	dBm	-66.2	-68.9	-71.8
Total noise power	Noise_total	dBm	-96.3	-87.1	-87.1
Interference power	P_interference	dBm	-94.5	-85.3	-85.3
Signal-to-noise ratio	SNR	dB	30.2	18.1	15.2
Signal-to-Interference-plus-noise ratio	SINR	dB	26.1	14.1	11.2

Capacity	C	Mbps	159.5	466.8	376.4
Throughput	Thput	Mbps	53.7	186.7	150.6
Base station antenna gain calculation:					
Antenna element gain		dBi	6.2	6.2	6.2
subarray gain		dB	3.0	7.8	7.8
array gain		dB	15.1	19.8	19.8
Antenna Gain	G_RX	dBi	24.2	33.8	33.8
Requirements					
User-experienced bitrate (requirement)		Mbps	25	120	120

Table 31 Analysis of uplink for the link from airborne UE to terrestrial base station

Parameter	**Symbol**	**Unit**	**5G**	**6G UAV**	**6G eVTOL**
System parameters:					
Carrier frequency	Freq	GHz	3.5	10	10
Channel Bandwidth	BW	MHz	20.0	100.0	100.0
DL Bandwidth used for calculations	BWeff	MHz	18.4	98.3	98.3
Transmitter side:					
Transmit power	P_out	dBm	49.0	53.0	53.0
Antenna Gain	G_TX	dBi	24.2	33.8	33.8
Cable loss, line losses, and switch losses	L_implementationTX	dB	2.0	2.0	2.0
Pointing losses	L_pointingTX	dB	1.0	3.0	2.0
Path:					
Total TX to RX distance		m	1525.0	1525.0	3154.5
Path loss	PL	dB	110.0	119.1	125.4
Atmospheric loss	L_atmos	dB	0.4	1.2	1.5
Rain and water evaporation attenuation	L_rain	dB	0.0	0.3	0.7
shadowing/fading margin		dB	3.0	3.0	3.0
Total path loss	PL_total	dB	110.4	120.7	127.6
Receiver side:					
Receive noise factor	Nf	dB	9.0	13.0	13.0
Metrics:					

Effective Isotropically Radiated Power	EIRP	dBm	70.2	81.8	82.8
Received signal power	S_RX	dBm	-40.2	-38.9	-44.8
Total noise power	Noise_total	dBm	-92.3	-81.1	-81.1
Interference power	P_interference	dBm	-87.6	-76.3	-76.3
Signal-to-noise ratio	SNR	dB	52.2	42.1	36.2
Signal-to-Interference-plus-noise ratio	SINR	dB	46.1	36.1	30.2
Capacity	C	Mbps	281.4	1179.6	986.4
Throughput	Thput	Mbps	109.8	587.7	587.7
Requirements					
User-experienced bitrate (requirement)		Mbps	50	100	100

Table 32 Analysis of downlink for the link from terrestrial base station to airborne UE